

Seismic assessment of Romanian Orthodox masonry churches in the Banat area through a multi-level analysis framework

Anna Lo Monaco^{a,*}, Nicola Grillanda^b, Iasmina Onescu^c, Mihai Fofiu^c,
 Francesco Clementi^d, Michele D'Amato^a, Antonio Formisano^e, Gabriele Milani^f,
 Marius Mosoarca^c

^a Department of European and Mediterranean Cultures, Architecture, Environment and Cultural Heritage (DiCEM), University of Basilicata, Via Lanera 20, Matera 75100, Italy

^b Department of Civil and Structural Engineering, University of Sheffield, Mappin Street, Sheffield S1 3JD, United Kingdom

^c Department of Architecture, Faculty of Architecture and Town Planning, Polytechnic University of Timișoara, Piața Victoriei 2, Timișoara 300223, Romania

^d Department of Civil and Building Engineering, and Architecture (DICEA), Polytechnic University of Marche, Via Breccia Bianche 12, Ancona 60131, Italy

^e Department of Structures for Engineering and Architecture, School of Polytechnic and Basic Sciences, University of Naples "Federico II", Piazzale Tecchio 80, Naples 80125, Italy

^f Department of Architecture, Built Environment and Construction Engineering (A., B., C.), Polytechnic University of Milan, Piazza Leonardo da Vinci 32, Milan 20133, Italy

ARTICLE INFO

Keywords:

Existing masonry churches
 Seismic risk
 Seismic vulnerability
 Failures mechanisms
 Kinematic limit analysis
 Modal analysis
 Push-over analysis

ABSTRACT

This paper aims to show some results of seismic assessment of Romanian Orthodox existing masonry churches, by extending the multi-level approach proposed by the Italian directive for seismic risk evaluation of cultural heritage. To this scope, a sample of six existing churches is examined, belonging to a church typology characterized by a single vaulted nave and a bell tower incorporated into the main façade. All churches considered in this study are located in the Banat region, which is an area with a medium–high seismic hazard.

Firstly, territorial Level of Valuations (LVO and LVT) are conducted on the churches sample examined. Afterwards, local (LV2) and global (LV3) valuations are performed on a case study, the Învierea Domnului church, assumed representative of all the churches sample under consideration. In particular, local analyses are performed on some church architectural portions with the kinematic limit analysis. Whereas, global analyses are conducted with non-linear push-over approach. Comments and comparisons of the obtained results are reported for each LV examined.

1. Introduction

Masonry churches represent an important part of the cultural heritage, being testimony of existing typologies with the related construction details largely applied in the past. To date, most of them are still normally used due to their important and social value played, even if they were not designed for seismic actions and, therefore, today they are extremely vulnerable also in moderate seismic areas. For this reason, recently the knowledge of existing masonry churches behaviour has become an important theme, in order to

* Corresponding author.

E-mail address: anna.lomonaco@unibas.it (A. Lo Monaco).

correctly predict the response and to design the structural interventions required.

To date in literature several works have been addressed on the seismic response of existing masonry churches. A first group of these works are addressed in debating on the seismic damage surveyed on churches due to recent earthquakes, in order to identify the most frequent response mechanisms [17,24,30,32,38,41,42,48,52,57]. All of these works confirm that, depending on the masonry typology investigated, seismic damage in existing masonry churches is recurrent in their construction parts called-macro-elements [17], as function of their geometrical configuration and construction details (façade, nave, triumphal arch, dome, bell tower, etc).

Moreover, several efforts have been made in order to properly numerically assess the seismic response of existing masonry churches, also considering response mechanisms observed during the recent earthquakes. To this regard, to date different Levels of Valuation (LVs) have been proposed. Some of them may be regarded as belonging to a unique multi-level framework such as the approach proposed in the Italian Directive for seismic risk evaluation of cultural heritage [28]. Of course, these LVs are characterized by the fact that the higher the LV the higher information number and computational costs required. The simplest LV is addressed to territorial evaluations, a tool particularly useful for owners and authorities in order to predict seismic damages scenarios. They estimate the seismic vulnerability starting from a global index correlated to several information of the churches or, more in general, of the constructions under considerations. Among these studies, one may refer to [19,21,22,34,35,54]. Moreover, the LVO proposed in [13,14,23], and the LV1 proposed in [28] are suitable for territorial scale seismic evaluations.

More refined analysis may be conducted on each church through a local seismic response evaluation. Coherently with this approach, usually a schematization in architectural parts (i.e. macro-elements) is made, in order to identify all the potential failure mechanisms under seismic lateral loadings. This approach, contemplated as LV2 by the Italian Directive [28], is developed starting from the kinematic linear and non-linear analysis, permitting as well to design the required interventions. To date, there are several works focused on this approach such as, among the others: [4,6,8,15,25–27,29,31,37,38,53,60].

Finally, the most refined approach is achieved if global models are implemented, or else local models where the interaction among the structural parts is correctly taken into account. Numerical simulations by means of Finite Element Models (FEMs) belong to this group, where commonly masonry is modelled as a continuum material having constitute non-linear relationships and a failure criterion. Also, the LV3 of the Italian Directive [28] falls within this approach. Of course, a global evaluation is valid if local response mechanisms are inhibited. Its applications may be found, among the others, in [10,55,59,62].

The work presented in this paper is part of a research focused on existing Romanian Orthodox masonry churches located in the Banat region [41–42], which is the second most important seismic area in Romania [45]. These churches are characterized by a particular structural configuration: they have a rectangular plan with a single nave, a circular or polygonal apse, and a bell tower centrally incorporated into the main façade. Similarly to the Italian ones [28], also for these churches previous works have shown that the seismic damage is localized in architectural parts, validating also in this case the macro-elements approach [43]. Fig. 1 depicts a

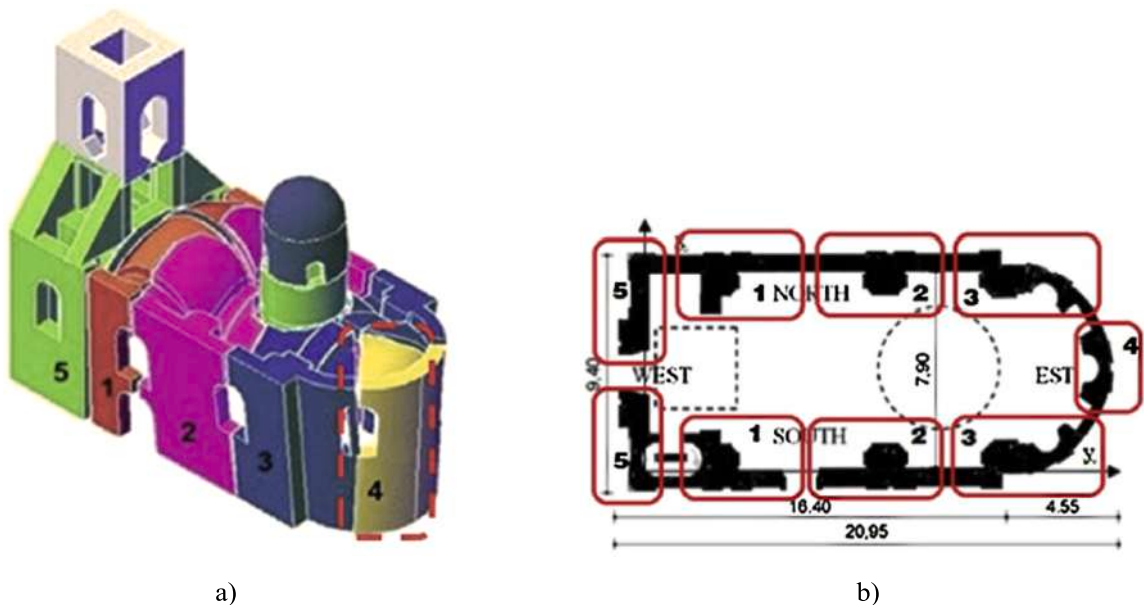


Fig. 1. Failure rigid blocks schematization: a) axonometric view; b) plan view.

division in rigid blocks (macro-elements) for existing Romanian Orthodox masonry churches investigated in [41,43]. Moreover, recent investigations have highlighted that in this area earthquakes with a significant vertical component occurred, resulting in severe damage on masonry structures, such as vertical shear cracks deriving from the differential vertical soil movements, that can furtherly facilitate out-of-plane collapses [7,44].

The aim of this study is to show the application of a multi-level methodology, in particular the one proposed by the Italian guidelines extended in this case to Romanian churches. This is due to the fact that Romanian churches behave similarly to the Italian ones, showing a damage for seismic lateral actions concentrated only in some architectural portions. To this scope, in this study six existing Romanian Orthodox masonry churches are investigated through different LVs. At first, *LV0* and *LV1* territorial evaluations are conducted in order to rank seismic performance within the churches sample considered. Then, according to the *LV2* approach, local failure response mechanisms are investigated with kinematic limit analysis tool as proposed in [8,27]. Finally, results of the *LV3* approach are shown, obtained through a Non-Linear Finite Elements Analysis (NLFEA) with a smeared crack-model for simulating cracks initiation and propagation within the existing masonry. The *LV2* and *LV3* results are presented for the case study of the Jesus Resurrection church (Înviearea Domnului), located in the Belinț municipality. This church is considered representative of all six Romanian Orthodox churches examined in this work. Moreover, the documents available (photographic documents, surveys, drawings, material details) for this church are sufficiently complete with the purpose of performing local (*LV2*) and global (*LV3*) seismic analyses.

2. Case studies






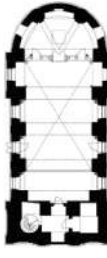

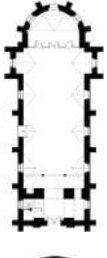

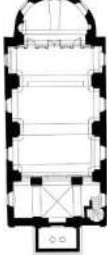
The case studies investigated are located in the Banat region of Romania, near Hungary and Serbia (Fig. 2). It was established in the 18th Century by the Habsburg Empire, and now it is a multicultural region, due to the past repopulation strategies and spontaneous migration of Romanians, Germans, Hungarians, Serbians, and others [33]. Currently, Timișoara is the capital, and the region is composed of two counties, Timiș and Caraș-Severin, even if in the past this area was larger, including Hungarian and Serbian lands [3].

Six churches are considered in this study, that are:





Fig. 2. Localization of the Banat area within Romania and Europe and localization of the six investigated churches.

Table 1
Principal information of the six investigated churches in the Banat region.

Church n°	Location	Name and year of construction	Picture	Plan	Wall thickness and tower height	Damages
1	Municipality of Cenad	Holy Spirit Descent church (Biserică Pogorărea Sfântului Duh) 1888			70–75 cm 26.15 m	cracks on the structural walls, damaged plaster and paintings
2	Municipality of Chizătău	Virgin Mary's Nativity church (Biserică Nașterea Maicii Domnului) 1827			57–97 cm 23.31 m	cracks between the tower walls and the longitudinal central nave walls, damaged plaster and paintings
3	Municipality of Bocșa	Saint Nicholas church (Biserică Sfântul Nicolae) 1795–1911			100–160 cm 35.33 m	damaged plaster and paintings
4	Municipality of Bencecu de Jos	Saint Nicholas church (Biserică Sfântul Nicolae) 1899			55–75 cm 23.27 m	cracks on the structural walls, damaged plaster and paintings
5	Municipality of Beregsău Mare	Saint George church (Biserică Sfântul Gheorghe) 1793–1810			35–75 cm 27.96 m	cracks on the structural walls, damaged plaster and paintings

(continued on next page)

Table 1 (continued)

Church n°	Location	Name and year of construction	Picture	Plan	Wall thickness and tower height	Damages
6	Municipality of Belinț	Jesus Resurrection church (Biserică Învierea Domnului) 1797			70–100 cm 25.80 m	vertical cracks in the apse area, damaged plaster and paintings

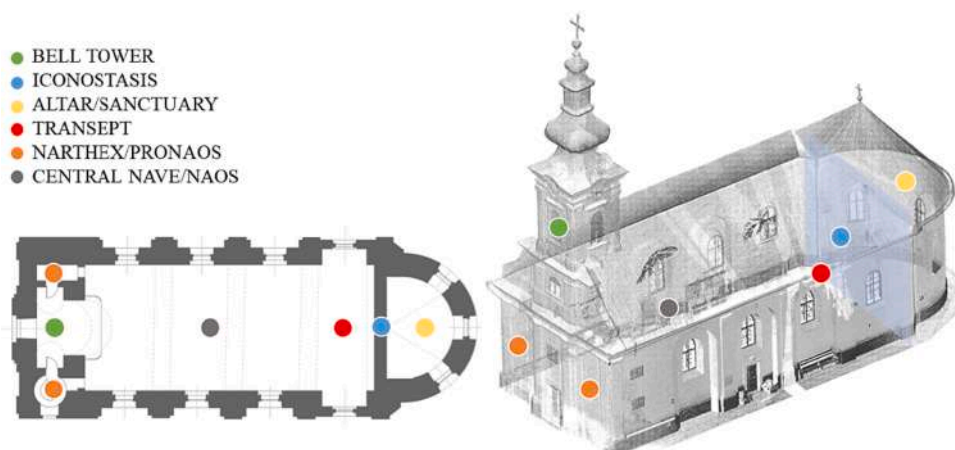


Fig. 3. A representation of a typical Romanian Orthodox masonry church in the Banat area.

1. “Holy Spirit Descent Church” (*Biserică Pogorârea Sfântului Duh*) - Municipality of Cenad;
2. “Virgin Mary’s Nativity Church” (*Biserică Nașterea Maicii Domnului*) - Municipality of Chizătău;
3. “Saint Nicholas Church” (*Biserică Sfântul Nicolae*) - Municipality of Bocșa;
4. “Saint Nicholas Church” (*Biserică Sfântul Nicolae*) - Municipality of Bencecu de Jos;
5. “Saint George Church” (*Biserică Sfântul Gheorghe*) - Municipality of Beregsău Mare;
6. “Jesus Resurrection Church” (*Biserică Învierea Domnului*) - Municipality of Belinț.

Five churches are located in Timiș county, in the municipalities of Cenad, Chizătău, Bencecu de Jos, Beregsău Mare and Belinț, while one of them is located in Caraș-Severin County, in the municipality of Bocșa, as presented in Fig. 2 [47].

Table 1 reports the investigated churches, with a representative picture, location, name, plan configuration, wall thickness and bell tower height, and principal damages currently observed.

From an architectural point of view, the selected case studies are representative of Romanian Orthodox masonry churches with an architectural typology of the XVIII-XIX Century in the Banat area. This church typology is characterized by a rectangular simple plan and a unique nave, covered by barrel vaults and arches, with a bell tower centrally positioned within the main façade. Gable or Dutch roof is recurrent for this church typology. The division of the interior space is specific of the Orthodox churches. The first main space is the *pronaos*, also called as narthex. It is followed by the main space, the *naos*, also called the central nave. The wall separating the naos from the altar is called *iconostasis* and is usually made of decorated wood. The last space is the altar, usually oriented to the East, named the *sanctuary* as well. A representation of a typical Romanian Orthodox masonry church is presented in Fig. 3 [42].

All the investigated buildings present a plan with a unique central nave, built in brick masonry with perimetral massive walls with thicknesses up to 160 cm. The most common damages observed on the investigated churches are due to lack of preservation in the past years, showing cracks on the structural walls, damaged plaster and paintings (Fig. 4).



Fig. 4. Exterior and interior pictures which show the conservation state of the investigated churches: a) Holy Spirit Descent Church of Cenad; b) Virgin Mary's Nativity Church of Chizătău; c) Saint Nicholas Church of Bocea; d) Saint Nicholas Church of Bencecu de Jos; e) Saint George Church of Beregsău Mare; f) Jesus Resurrection Church of Belinț.

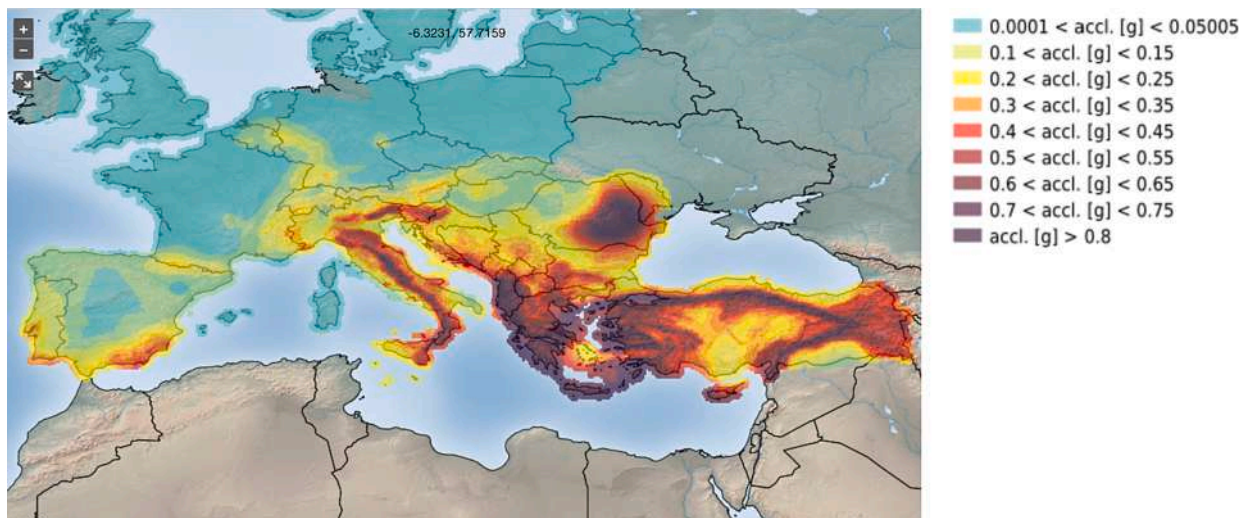


Fig. 5. ESHM20 maps for $Sa(0.2\text{ s})$ [16].

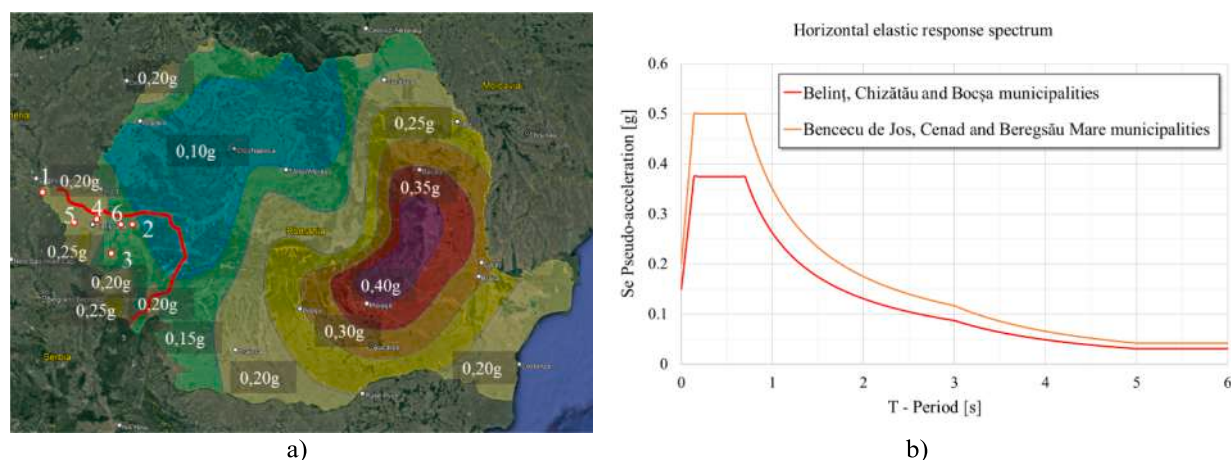


Fig. 6. a) expected ground acceleration a_g and b) horizontal seismic action elastic spectra for *LSLS*, according to [56].

2.1. Seismicity of the area

Romania is characterized by a moderate seismic hazard with respect to the other countries in Europe. As proof of this, Fig. 5 reports the pseudo-spectral acceleration S_a associated to a vibration period equal to 0.2 s [$S_a(0.2\text{ s})$] according to the 2020 European Seismic Hazard Model - ESHM20, [63], for a reference rock site conditions (A class according to [18], with a Probability Of Exceedance (POE) of 10% in 50 years. From this map it can be noted that Romania is located in an area with a medium–high seismicity, lower than some others of Europe.

In detail, two significant seismic areas may be found in Romania, that are Vrancea (in the middle east) and Banat (western), the latter considered in this study. The Vrancea seismic area is characterized by intermediate depth earthquakes, with the most significant seismicity registered in the bending zone of the Eastern Carpathian arch. In this area, 2–3 earthquakes per century with a magnitudes M_w over 7 are registered [2]. Whereas, the Banat region is located on the border with Hungary and Serbia, where more than 600 earthquakes were registered since 1773, and six of them had a magnitude $M_w = 5.0$ – 5.7 [64]. It is characterized by shallow earthquakes of crustal type, with focal depths between 1 and 35 km and epicentres in the entire Banat region [1].

Fig. 6 reports, according to the [56], the expected ground acceleration a_g (Fig. 6a) and the resulting horizontal elastic spectra of the seismic action (behaviour factor $q = 1$) for Life Safety Limit State (*LSLS*) (Fig. 6b). They refer to the different municipalities of the churches, for 225 years mean return period (20% in 50 years probability of exceedance), and by assuming an Importance factor $\gamma_I = 1$. In particular, for Belinț, Chizătău and Bocșa municipalities where Jesus Resurrection Church, Virgin Mary's Nativity Church and Saint Nicholas Church are respectively located, the expected ground acceleration $a_g = 0.15\text{ g}$. Whereas, for Bencecu de Jos, Cenad and Beregsău Mare municipalities where Saint Nicholas Church, Holy Spirit Descent Church and Saint George Church are respectively located, $a_g = 0.20\text{ g}$. In all the municipalities the reference periods for the spectrum are $T_B = 0.14\text{ s}$, $T_C = 0.7\text{ s}$, and $T_D = 3\text{ s}$.

It should be noted that to date a hazard law in the current Romanian design code is not available. Moreover, it is also difficult to correlate the expected ground acceleration a_g (horizontal and vertical) to the return period. This issue is still open, and deserves to be investigated more in detail in the future [49–51].

3. Territorial scale assessment

The goal of this section is to illustrate two different simplified methods for assessing the seismic vulnerability on existing churches, applied to the six case studies chosen in this work. A territorial seismic assessment is implemented with the aim of estimating a priority scale for the existing churches considered.

3.1. LVO method

In this paragraph the application on the six case studies of a simplified method for the seismic assessment at a territorial level is shown. This Level of Valuation, that is briefly indicated as *LVO*, is a qualitative assessment tool that does not require any on-site investigation and quantitative information for its application [13,14,23]. Due to its simplicity, this method allows obtaining a fast appraisal of the churches' seismic performance, useful for ranking priorities and planning further investigations with more refined methods. It is briefly identified as *LVO* [14], since it may be easily implemented before the *LV1* in the multi-level approach proposed by the Italian Directive [28].

The LVO required the evaluation of the three scores related to Hazard (*H*), Vulnerability (*V*) and Exposure (*E*) to define the seismic risk score *R* according to the following equation [20,61].

$$R = H \cdot V \cdot E \tag{1}$$

However, a LVO simplified application may be obtained without the exposition value *E* of the church, according to the following expression [14]:

$$R = [H + 1] \cdot V \tag{2}$$

where the *H* score is being added to unity for obtaining a seismic risk score *R* greater than one. This simplified application is used in this paper.

The Hazard score *H*, is a dimensionless parameter, calculated according to Eq. (3). It considers a maximum of 11 environmental threats [23], that may be divided in *sporadic events* (seismic action, landslides or faults, volcanic threat, hydro-meteorological threat, chemical-technological threat, and forest-fire) and *continuous processes* (erosion, physical stress, air pollution, socio-organizational, and demographic decline).

$$H = \sum_{k=1}^{11} h_{k,i} \tag{3}$$

Table 2 reports for each threat considered the damage severity score $h_{k,i}$ assigned, where *k* is the *k*th threat, and *i* is the *i*th damage severity (*i* = 1, 2, 3 corresponding to no damage/no hazard, low or gradual, Catastrophic). The potential damages may be estimated by collecting information reported in existing documents regarding the same threat occurred in the past, or else by using predicting models.

Whereas, the Vulnerability score *V* is given by the weighted sum of 13 parameters related to the building properties, such as structural characteristics, conservation status and building position. In details, the parameters considered are: position of the building and foundations, floor plan configuration or geometry, elevation configuration, distance between walls, non-structural elements, type and organization of the resistant system, quality of the resistant system, horizontal structures, roofing configuration, conservation status, environmental alterations, construction system alterations, fire vulnerability. To each of these parameters a vulnerability level A, B, C, or D may be assigned, where A corresponds to an absent (or very low) and D to a very high vulnerability.

The Vulnerability score *V* is given by the following expression:

$$V = \sum_{k=1}^{13} \rho_k v_{k,i} \tag{4}$$

where $v_{k,i}$ is the score of the vulnerability level assigned of the *i*th parameter, and ρ_k is the related weight. Table 3 reports the vulnerability scores and the related weights.

Appendix A reports, for each of the six churches considered in this study, the values assigned for calculating the resulting Hazard *H* and the Vulnerability *V* score (from Tables 6-11). They are plotted in the histogram of Fig. 7, together with the resulting Risk score *R*, listed in descending order. The highest *R* score is found in the case of the Holy Spirit Descent church (biserică Pogorârea Sfântului Duh) located in the municipality of Cenad. On the contrary, the lowest *R* score is obtained in Jesus Resurrection Church (biserică Învierea Domnului) in the Belinț municipality. As one may note the resulting risk *R* depends on the combination of the two scores estimated (that are *H* and *V*). Moreover, the church with the lowest seismic risk *R* score (Jesus Resurrection Church) has not the lowest vulnerability *V* score (*V* = 29.63 obtained for the Saint Nicolas church), since the latter church is located in an area having the highest seismic hazard *H* among the ones considered in this study.

Table 2
Seismic hazard scoring [14,23].

Threats	Severity of damage $h_{k,j}$				
		No damage/ No hazard	Low or gradual	Catastrophic	
<i>Sporadic events</i>	1	Seismic action	0	0.20	0.40
	2	Landslide or rock fracture	0	0.15	0.25
	3	Volcanic threat	0	0.20	0.40
	4	Hydro-methodological threat	0	0.15	0.25
	5	Chemical–technological threat	0	0.15	0.25
<i>Continuous processes</i>	6	Forest fire	0	0.15	0.25
	7	Erosion	0	0.05	0.10
	8	Physical stress	0	0.05	0.10
	9	Air pollution	0	0.01	0.05
	10	Socio-organizational	0	0.01	0.05
	11	Demographic decline	0	0.01	0.05

Table 3
Scores and weights for seismic vulnerability evaluation [23,14].

	Parameter	Vulnerability $v_{k,i}$				Weight
		A	B	C	D	ρ_k
1	Position of the building and foundations	0	1.35	6.73	12.12	0.75
2	Floor plan configuration or geometry	0	1.35	6.73	12.12	0.5
3	Elevation configuration	0	1.35	6.73	12.12	1.0
4	Distance between walls	0	1.35	6.73	12.12	0.25
5	Non-structural elements	0	1.35	6.73	12.12	0.25
6	Type and organization of the resistant system	0	1.35	6.73	12.12	1.5
7	Quality of the resistant system	0	1.35	6.73	12.12	0.25
8	Horizontal structures	0	1.35	6.73	12.12	1.0
9	Roof configuration	0	1.35	6.73	12.12	1.0
10	Conservation status	0	1.35	6.73	12.12	1.0
11	Environmental alterations	0	1.35	6.73	12.12	0.25
12	Construction system alterations	0	1.35	6.73	12.12	0.25
13	Fire vulnerability	0	1.35	6.73	12.12	0.25

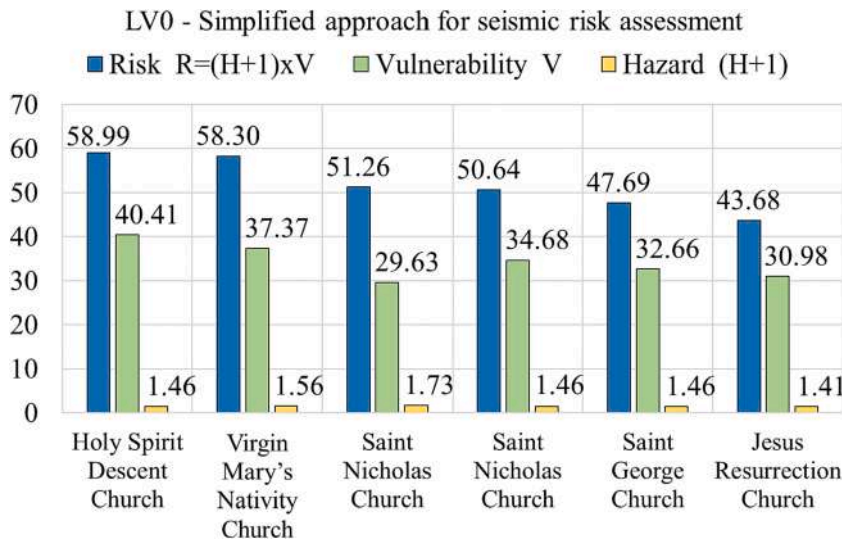


Fig. 7. LV0 results of the six case studies considered.

3.2. LV1 method

The LV1 proposed by [28], permits evaluating the seismic performance at a territorial level, correlating the ground acceleration a_g to a vulnerability global index i_v , which ranges from 0 to 1. This approach involves a qualitative vulnerability evaluation of 28 response mechanisms, taking into account as well the presence of useful seismic devices. All the response mechanisms may be found in [28].

The vulnerability global index i_v is calculated as follows:

$$i_v = \frac{1}{6} \cdot \frac{\sum_{k=1}^{28} \rho_k \cdot (v_{ki} - v_{kp})}{\sum_{k=1}^{28} \rho_k} + \frac{1}{2} \tag{5}$$

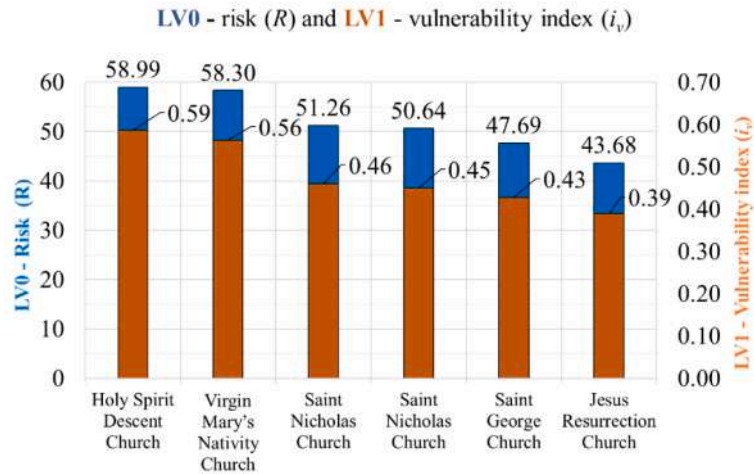
where ρ_k is the weight of response mechanism considered, 0 if not present, or ranging between 0.5 and 1 depending on the mechanism; v_{ki} (0, 1, 2 or 3) is the score assigned for the k^{th} mechanism and related to the estimated vulnerability; while v_{kp} (0, 1, 2 or 3) is the score assigned for the k^{th} mechanism related, instead, to the seismic-resistant device [28].

Once i_v is calculated, a ground acceleration a_g may be estimated. According to the Italian Directive [28], a_g may be estimated for Damage Limit State (DLS) and Life-Safety Limit State (LSLS). In particular, for LSLS, a_g is given by the following equation:

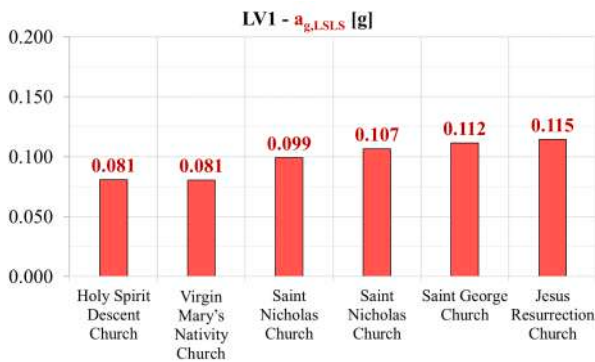
$$a_{LSLS} = 0.025 \cdot 1.8^{5.1-3.44i_v} [g] \tag{6}$$

where S is the stratigraphic amplification depending on the foundation soil.

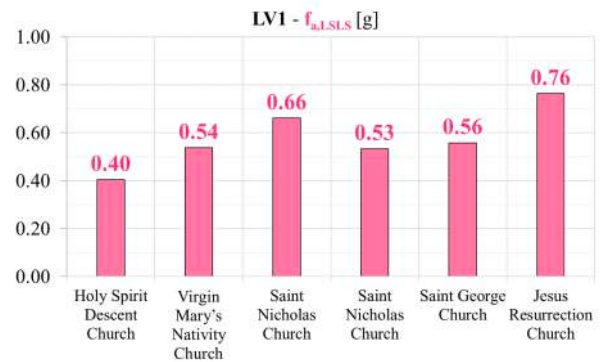
In addition, the acceleration factor for the LSLS $f_{a,LSLS}$ results from the ratio between the ground acceleration a_{LSLS} corresponding to the LSLS achievement (capacity) and the expected one $a_{g,LSLS}$, (demand), as follows:



a)



b)



c)

Fig. 8. a) LV0 and LV1 results comparison; b) the calculated LSLs acceleration $a_{g,LSLS}$; c) the calculated LSLs acceleration factor $f_{a,LSLS}$ for each church.

$$f_{a,LSLS} = \frac{a_{LSLS}}{a_{g,LSLS}} \tag{7}$$

Fig. 8a plots, in the histogram form, the vulnerability global index i_v for each church considered, while the value assigned to ρ_k , ν_{ki} and ν_{kp} are reported in the Appendix B, from Tables 12–14. In the same histogram the seismic risk score R previously calculated with the LV0 is reported, too. As one may note, a clear relative correspondence between R and i_v is obtained in the cases analysed. For completeness, Fig. 8b summarizes a_{LSLS} calculated with the Eq. (6), by dividing it for the amplification factor S . It is obtained by assuming for all churches a class C for subsoil category, and T1 as for the topographic category, according to the following equation [46]:

$$S = S_T \cdot S_S = 1 \cdot \left(1.7 - 0.6 \cdot F_0 \cdot \frac{a_g}{g} \right) \tag{8}$$

where, F_0 is the maximum dynamic amplification factor of the horizontal acceleration, whose value is 2.5 according to Romanian code. S_S and S_T are respectively function of subsoil category and topographic category.

In this case, the amplification factor for horizontal actions is supposed to be $S = 1.475$ if related to a peak ground acceleration $a_g = 0.15$ g and $S = 1.400$ for $a_g = 0.20$ g. A Confidence Factor (CF) = 1.35 is assumed in all the churches considered.

Finally, Fig. 8c reports the acceleration factor f_a calculated for each church.

As expected, there is a close correlation between a_g and i_v . A higher vulnerability index corresponds to a lower seismic capacity of the structure, and vice versa. According to the LV1 approach, it results that the church with the best seismic performance is still the Jesus Resurrection Church, as found by applying the LV0 approach. Moreover, the LV0 (Fig. 7) and the LV1 (Fig. 8) results are in agreement in ranking the seismic performance of the churches considered.

4. Seismic analyses on Jesus Resurrection church

In this section, the seismic assessment conducted via LV2 and LV3 methods is presented for Jesus Resurrection church (Învierea Domnului) located in the Belinț municipality. As previously introduced, this church may be considered as representative of all the six existing Romanian Orthodox masonry churches investigated at a territorial level located in the Banat region. The LV2 method is applied by following a numerical procedure of kinematic limit analysis recently applied to several historical masonry structures. Then, numerical global analyses provided by the LV3 method are performed via modal and static non-linear analyses on a FEM model of the whole church considered.

4.1. LV2 method: Kinematic limit analysis of local mechanisms

As previously mentioned, the LV2 method provides the evaluation of the seismic vulnerability through assessment of local response mechanisms of architectural parts (macro-elements), where rigid macro-blocks are considered subjected to a distribution of horizontal loads proportional to masses. In the selection of the possible seismic-induced local failures, in this study the subdivision into macro-elements suggested in [43] is taken into account, paying attention to the aula arches, façade and bell tower.

The numerical method adopted in this study is a computational kinematic limit analysis using a geometrical representation of the involved macro-blocks through NURBS parametric functions [53]. The main advantage of a NURBS-based kinematic approach is the possibility to evaluate mechanisms in which blocks can have any curved shape, both in the two- and the three-dimensional case. Each block is assumed infinitely rigid. At interfaces between adjacent elements, the standard no-tension material hypotheses can be assumed, i.e. no tensile resistance, infinite compression and shear strength [29]. Alternatively, finite ultimate stress values can be considered by defining a yielding surface (e.g. a simple conic Mohr-Coulomb domain or a homogenized failure surface [37]) together

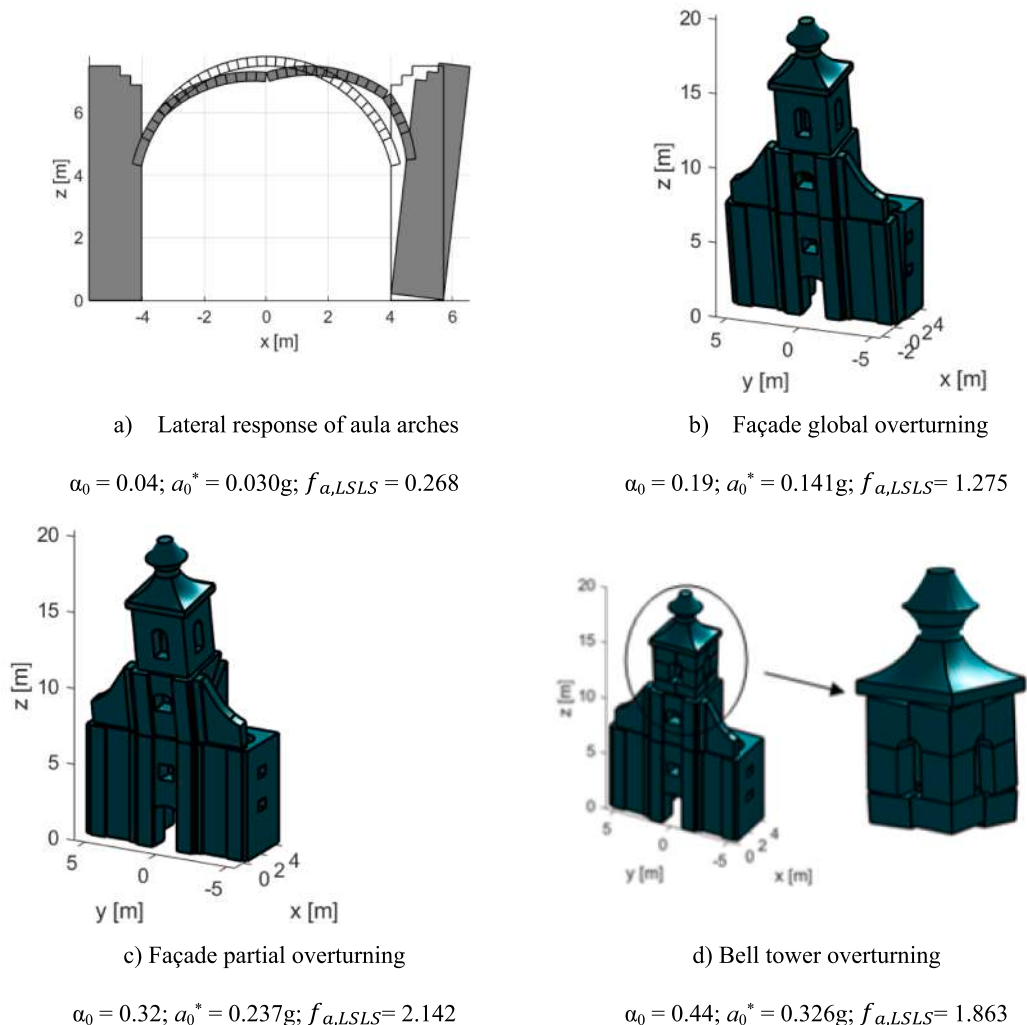


Fig. 9. LV2 for Jesus Resurrection church: (a) collapse of the arch in the central nave, (b) façade global and (c) partial overturning, (b) belfry failure.

with the assumption of perfectly plastic behaviour. The overall limit analysis problem can be written in terms of a linear programming problem in which the main kinematic variables are the velocities of elements' centroids in the 3D space. The objective function is given by the minimization of the kinematic load multiplier, which is defined by imposing the balance between the external power given by loads and the internal power deriving from the stress along interfaces. Loads can be subdivided in terms of dead loads, i.e. the permanent loads deriving from self-weight and applied masses, and live loads, which are defined as a distribution of horizontal load proportional to masses and depending on the kinematic load multiplier. Constraints include the compatibility constraints, which express the associated flow rule depending on the material behaviour assumed at the interfaces, and the normalization of the power associated with live loads. The solution of the linear programming problem consists of a set of translational and rotational velocities and defines the mechanism to which the minimum kinematic multiplier α_0 is associated, by means of the following expression:

$$\min\{\alpha_0 \mathbf{f}_L^T \mathbf{u} = -\mathbf{f}_D^T \mathbf{u} + \mathbf{c}^T \mathbf{p}\} \text{ such that } \begin{cases} \mathbf{A}_{comp} \begin{bmatrix} \mathbf{u} \\ \mathbf{p} \end{bmatrix} = 0 \\ \mathbf{f}_L^T \mathbf{u} = 1 \\ \mathbf{p} \geq 0 \end{cases} \quad (9)$$

in which α_0 is the horizontal plastic multiplier; \mathbf{f}_D and \mathbf{f}_L are the dead and live loads vectors, respectively; \mathbf{u} is the centroid velocities vector; \mathbf{p} collects the non-negative plastic multiplier rates (which is unknown together with \mathbf{u} in the linear programming problem); \mathbf{c} is the vector allowing to compute the internal dissipated power; and the matrix \mathbf{A}_{comp} defines the compatibility constraints (i.e. assuring that the flow rule is respected). Further details on the method can be found in [26]. Through the research works conducted in the recent years, this approach has proven to be suited for evaluation of local mechanisms in historical masonry structures. In particular, some applications on churches can be found in [8,27].

Once mechanism (\mathbf{u}) and horizontal load multiplier α_0 are known, simple calculations can be used to evaluate the corresponding capacity, quantified in terms of spectral acceleration α_0^* calculated by applying the standard modal [28,40]:

$$\alpha_0^* = \frac{\alpha_0 \sum w_i}{M^* FC} \quad (10)$$

Once, the capacity α_0^* is known, for LSLS it must be verified that:

$$\alpha_0^* > \alpha_{0min}^* \quad (11)$$

α_{0min}^* is the demand in terms of spectral acceleration, depending on whether the response mechanism is ground-connected or, else, it arises at a certain height, calculated as:

$$\alpha_{0min}^* = \begin{cases} \frac{a_g(P_{VR}) \cdot S}{q} \text{ for ground connected mechanisms} \\ \max\left\{ \frac{a_g(P_{VR}) \cdot S}{q}; \frac{S_e(T_1) \cdot \psi(z) \cdot \gamma}{q} \right\} \text{ otherwise} \end{cases} \quad (12)$$

where w_i are the dead weights (they coincide with the translational vertical components in the load vector \mathbf{f}_D); M^* is the effective participating mass, evaluated as $M^* = \frac{(\sum w_i u_{hi})^2}{g \sum w_i u_{hi}^2}$ (in which u_h is the horizontal component of the point on which the mass is lumped and

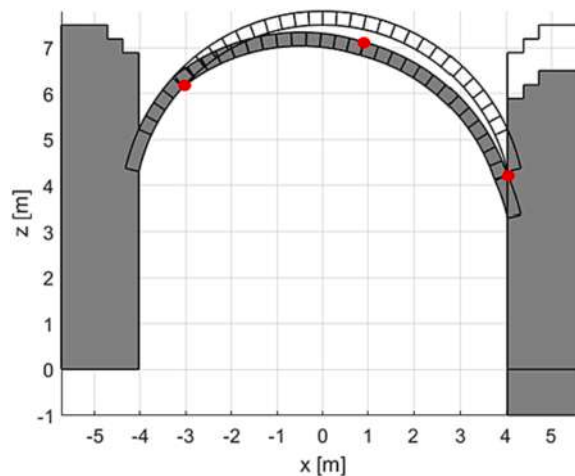


Fig. 10. Jesus Resurrection church. Analysis of the arch subjected to differential vertical settlements: deformed structure scaled by 100 (vertical displacement applied equal to 1 cm).

g is the gravity acceleration); q is the behavior factor assumed equal to 2; T_1 is the fundamental period estimated equal to $0.07H_e^{0.75}$ for churches (in which H_e is the height); $\psi(z) = \frac{z}{H}$ is assumed as shape of the first vibration mode; $\gamma = 3N/(2N + 1)$ is the modal participating coefficient (with N the storeys number); and finally CF is the Confidence Factor assumed equal to 1.35.

Finally, the acceleration factor $f_{a,LSLS}$ in terms of spectral accelerations may be calculated as follows:

$$f_{a,LSLS} = \frac{a_0^*}{a_{0min}^*} \tag{13}$$

As for the Jesus Resurrection church (Învierea Domnului) considered in this study, Fig. 9 the response mechanisms considered with the related numerical results. Given the complexity of geometries, a modelling strategy via NURBS solids [26] is used here. In particular, the following mechanisms are evaluated: lateral response of aula arches (Fig. 9a); façade global overturning (Fig. 9b); façade partial overturning (Fig. 9c); belfry overturning (Fig. 9d). In all the cases, the limit behaviour of masonry is characterized by a null tensile strength and finite values for compression and shear resistances. The compression strength is set equal to 2.35 MPa, according to the value measured in a previous investigation [1], where compression tests were carried out on specimens of masonry similar to the one under consideration. Whereas, the shear response is ruled by a Mohr-Coulomb frictional behaviour by assuming a friction angle tangent of 0.4, in agreement with the Italian regulations [9] for similar masonry. Finally, a small cohesion equal to 0.05 MPa is assigned to avoid numerical instabilities. 18 kN/m^3 is assigned as specific weight. The arch is considered supported by two abutments whose thickness coincides with the thickness of the longitudinal nave walls, whereas the presence of the barrel vault has been included through a distributed mass at the extrados of the arch.

For the response mechanisms considered different results are found. In particular the most vulnerable response mechanism is represented by the lateral response of aula arches, where the capacity in terms of spectral acceleration a_0^* is 0.030 g, $f_{a,LSLS} = 0.268$ corresponding to a ground acceleration $a_{g,LSLS} = 0.040 \text{ g}$. This result derives mainly from the slenderness of the arch compared with the

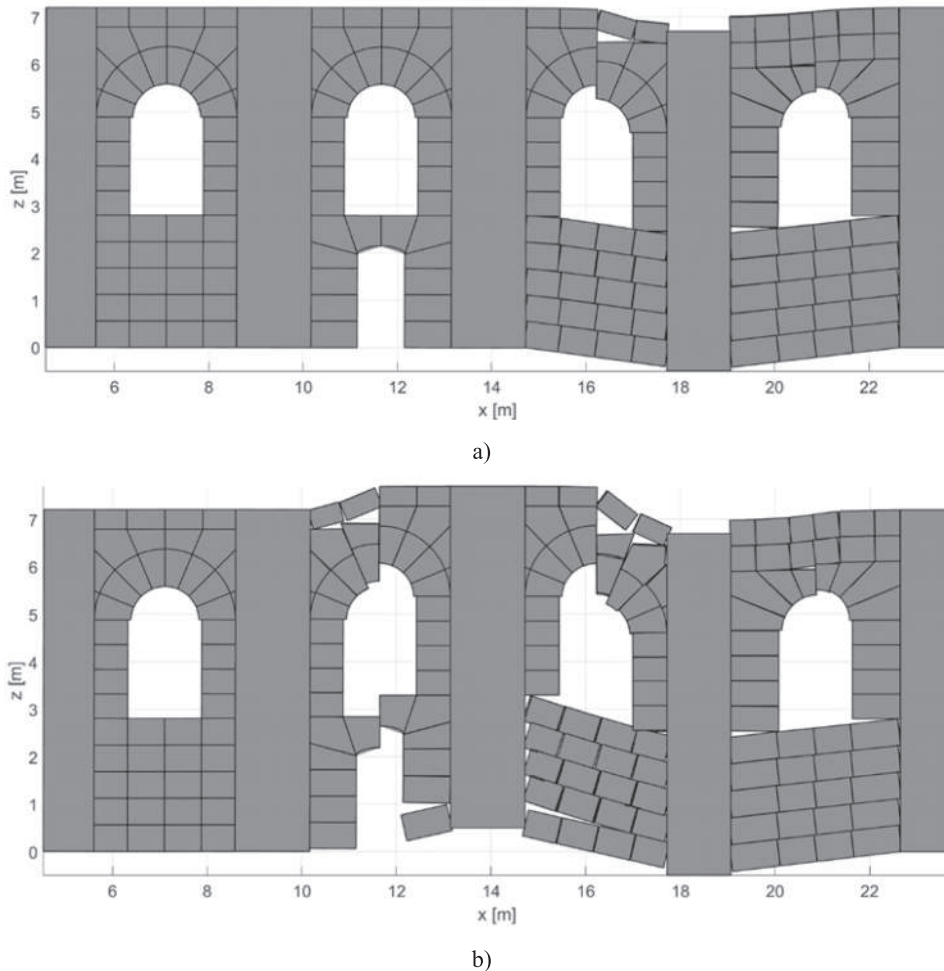


Fig. 11. Jesus Resurrection church. Analysis of the nave wall under vertical settlements, deformed structures scaled by 50 (maximum displacement applied equal to 1 cm): (a) bi-linear and (b) piecewise linear settlement configuration.

size of piers, whose overturning naturally leads the arch to collapse. Where, the least vulnerable mechanism is the Façade partial overturning with $a_0^* = 0.237$ g, $f_{a,LSLS} = 2.142$, $a_{g,LSLS} = 0.321$ g. These values significantly differ from the ones obtained in the case of LV1 analysis where a value of $a_{g,LSLS} = 0.115$ g was found. This result demonstrates that a global evaluation is only a fast tool for screening and comparing at a territorial level several churches. But, anyway, local analyses are unreplaceable in order to identify the most vulnerable mechanisms, that may vary case-by-case depending on local conditions.

In addition to the assessment of local mechanisms under horizontal load, some numerical simulations aimed at investigating the effects of a vertical seismic component are here reported. With particular reference to the surface waves due to near-field earthquakes, a first approximated cracks pattern associated to a vertical excitation can be obtained by modelling the differential soil movement as a vertical settlement at the base [44]. According to a limit analysis, devoted numerical tools based on the static or the kinematic method can be used [31,60]. Therefore, the above-mentioned kinematic approach has been followed to identify the structural response of some selected macro-blocks subjected to a differential vertical settlement at the base. The linear programming problem can be easily adapted by using displacements and rotations of centroids as main kinematic variables and introducing the work of the vertical reactions computed for the imposed base displacements in the balance of virtual works. Being referred to specific structural partitions, these analyses can be still considered as part of the LV2 methods.

Fig. 10 reports the result obtained for the arch in the central nave, in which a differential displacement for the two nave walls has been considered. The arch deforms by presenting three cylindrical hinges, as expected in previous research [60]. Fig. 11 shows the in-plane analysis of the nave wall. In order to represent surface waves with different wavelength, two different settlement configurations have been studied here: a bilinear negative displacement with minimum values on the fourth column (Fig. 11a), and a piecewise linear displacement (Fig. 11b). The material resistance parameters are the same used for the previous analyses. However, in order to allow using a mesh composed of a few quasi-regular rigid blocks and keeping low the computational effort, the internal dissipation is computed in different way for horizontal and vertical interfaces. Horizontal interfaces are considered representative of mortar joints, as well as inclined interfaces along the arches, and the simple Mohr-Coulomb behaviour is assigned to them. Along vertical interfaces, a not null tensile strength evaluated according to the homogenization theory presented by de Buhan & de Felice [5] is used in order to represent the interlocking between bricks in a running bond texture. Finally, a non-associative behaviour has been assigned in shear to exclude dilatancy effects [25]. The obtained results show the presence of vertical cracks, with some of them due to the shear effect. It is interesting to mention that some vertical cracks have been actually observed on the nave walls close to the transept. This case deserves several and more detailed investigations, thus the results here presented can be considered a starting point for more extended future research.

4.2. LV3 method: Global static non-linear analysis

A FEM numerical model of the Jesus Resurrection church (Învierea Domnului) is implemented within the MIDAS FEA NX© software [12] in order to perform linear modal and static non-linear (pushover) analyses. The numerical model (Fig. 12) is implemented according to the following criteria:

- the sloping wooden roof is not modelled for simplicity but considered only as distributed vertical load acting at walls top. In the modal analyses, this load and the roof elements self-weight is converted into the corresponding mass;
- belfry and the mezzanine floor made of wooden material are modelled with linear material;
- elements mesh takes into account variations in thickness and geometry, as in the case of curved vaults, and also the presence of windows;
- the church is fixed at the base of the vertical walls.

The existing brick masonry is modelled through a smeared crack-model for simulating cracks initiation and propagation within the

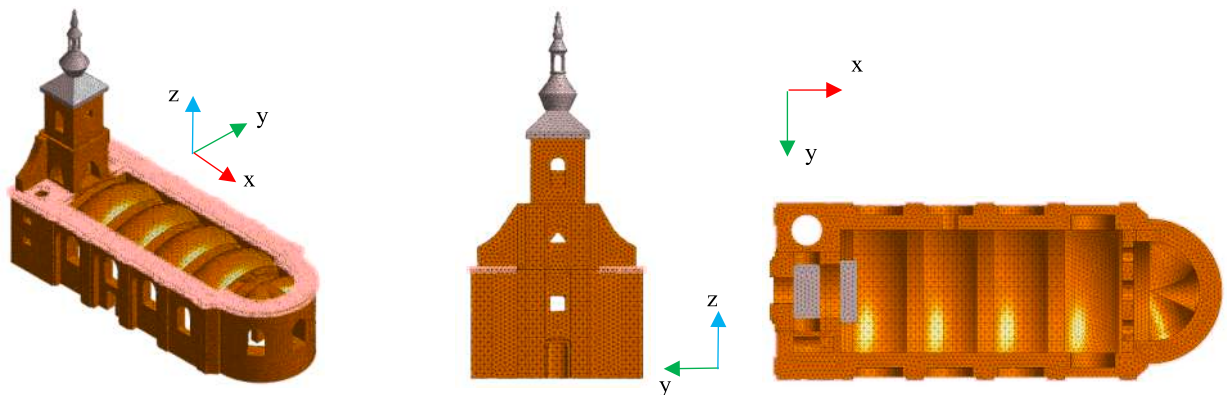


Fig. 12. Jesus Resurrection church (Învierea Domnului) FEM model.

Table 4
Brick masonry and softwood mechanical properties.

Brick masonry properties		Softwood properties ¹	
Model type: Concrete smeared crack - Isotropic		Model type: Elastic - Isotropic	
ρ Density (kg/m ³) ²	1800	ρ Density (kg/m ³)	290
E Normal elastic modulus (MPa) ²	2350	E Normal elastic modulus (MPa)	7000
G Tangential elastic modulus ²	940	G Tangential elastic modulus	440
ν Poisson's ratio	0.25	h Mesh size (mm)	300
f_c Compressive strength (MPa) ²	2.35		
f_t Tensile strength (MPa)	0.235		
G_c Compressive fracture energy (N/mm) ³	3.760		
G_f Tensile fracture energy (N/mm) ⁴	0.007		
h Mesh size (mm)	300		

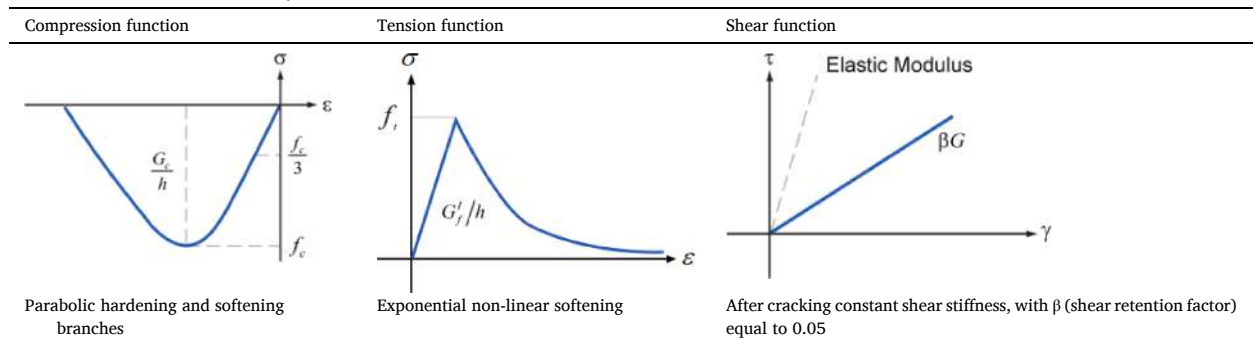
¹ Assumed conifer wood in C14 Class (UNI EN 338-2016).

² Properties obtained by means laboratory tests [1].

³ Calculated by means the equation $d_{u,c} = G_c / f_c$, assuming $d_{u,c} = 1.6$ mm [11].

⁴ Calculated by means the equation $d_{u,t} = G_f / f_t$, assuming $d_{u,c} = 0.029$ mm and $f_t = 10\% f_c$ [11].

Table 5
Functions considered for masonry smeared crack model.



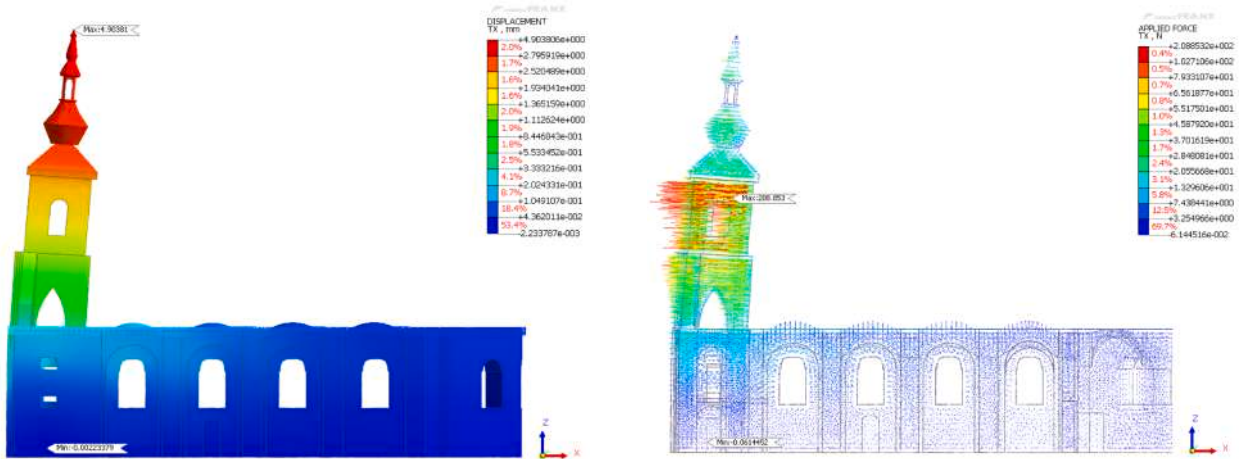
elements. A shear retention factor $\beta = 0.05$ is adopted, in order to attribute an after-cracking shear stiffness [10,36]. In this case, the following assumptions are made for the material relationships: a parabolic stress–strain in compression; a linear stress–strain in tension until the fracture, with an exponential non-linear softening; a linear relationship among shear stress and shear strain. Mechanical properties assigned to masonry and wood are summarized in Table 4, while the functions considered for the smeared crack model are reported in Table 5 [12].

A modal analysis is preliminarily performed. In particular, for sake of brevity Fig. 13 illustrates the results of the vibration Modes n. 1, n. 2 and n. 6. For each vibration mode considered the mode shape is reported together with the corresponding static inertial nodal forces resulting from a spectral analysis. The Mode n. 1, along X direction, is a local mode involving the bell tower within the main façade ($T_1 = 0.187$ s, $\%Mass_1 = 14.12\%$). The Mode n. 2 ($T_2 = 0.148$ s) and n. 6 ($T_6 = 0.079$ s) are global vibration modes along, respectively, Y (transverse direction) and X (longitudinal direction) having the highest participation mass percentages ($\%Mass_2 = 56.78\%$, $\%Mass_6 = 45.57\%$).

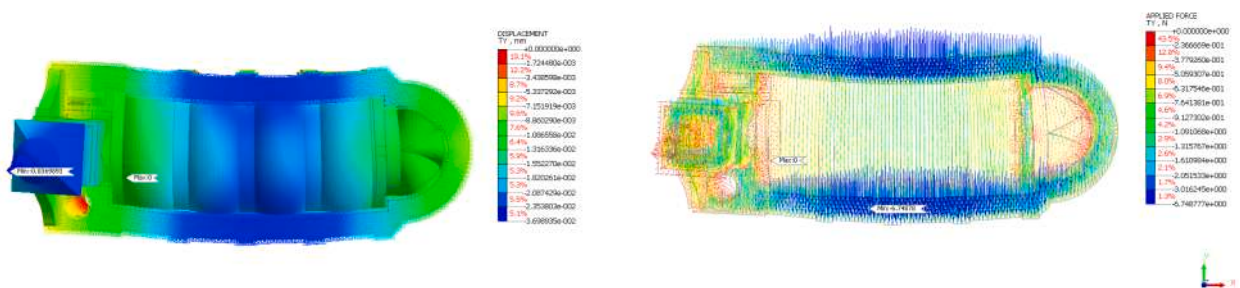
Then, Non-Linear Pushover Analyses (NLPAs) are performed along the two principal directions (X and Y) by using a lateral force distribution corresponding to the static inertial nodal forces of the Mode n. 6 for NLPAs along X direction, and of the Mode n. 2 for NLPAs along Y direction [12]. All the analyses are conducted in displacement control, by using an iterative procedure with a Newton-Raphson modified as for calculating non-linear solution. In details, the following criteria are set:

- load steps and intermediate output request: 50, every increment;
- convergence criteria/error tolerance: displacement (U) assumed 0.1;
- iteration method: displacement control method with a master node;
- maximum displacement: 100 mm (drift of 0.6%);
- stiffness update scheme: modified Newton-Raphson (recalculation of the stiffness matrix at the first iteration of each load increment, constant during the correction phase);
- maximum number of iterations per increment and maximum bisection level: 50 and 5.

a) Mode n. 1 ($T_1 = 0.187$ s, $\%Mass_1 = 14.12\%$)



b) Mode n. 2 ($T_2 = 0.148$ s, $\%Mass_2 = 56.78\%$)



c) Mode n. 6 ($T_6 = 0.079$ s, $\%Mass_6 = 45.57\%$)

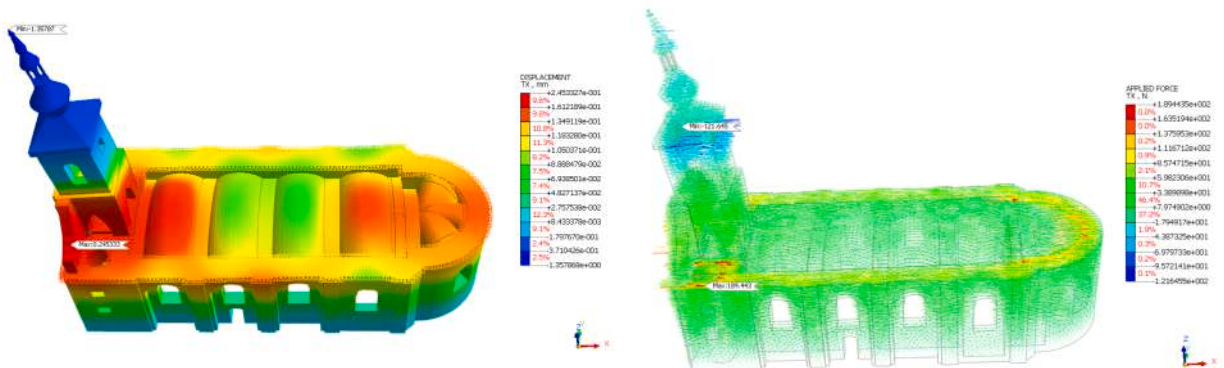
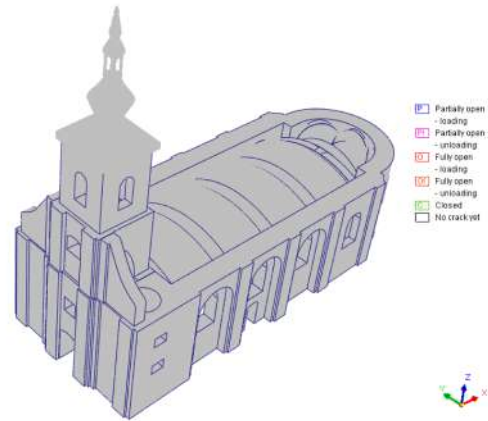
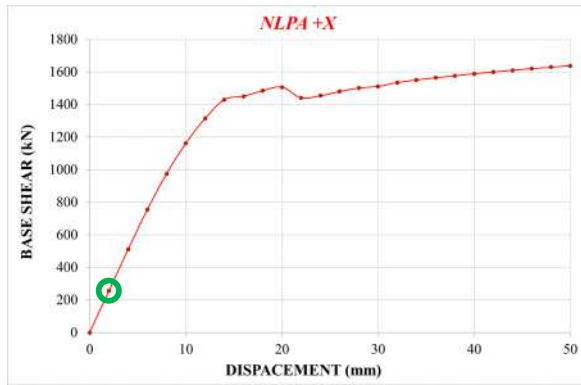
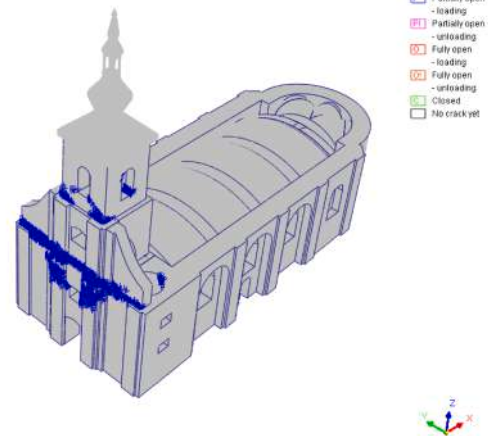
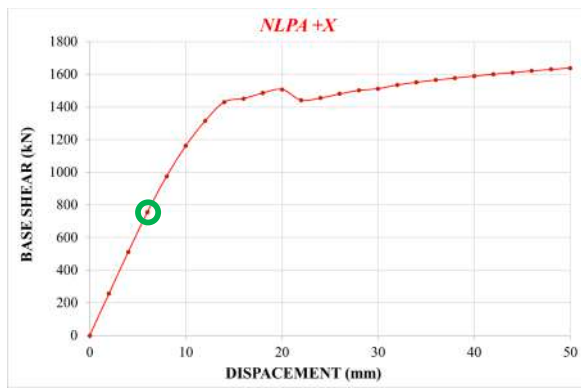


Fig. 13. Vibration mode shapes and Static inertial nodal forces: a) Mode n. 1, b) Mode n. 2 and c) Mode n. 6.

1st LOAD INCREMENT – *NLPA+X*



3rd LOAD INCREMENT – *NLPA+X*



11th LOAD INCREMENT – *NLPA+X*

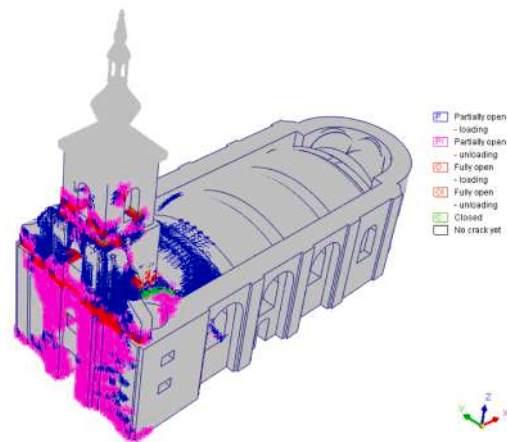
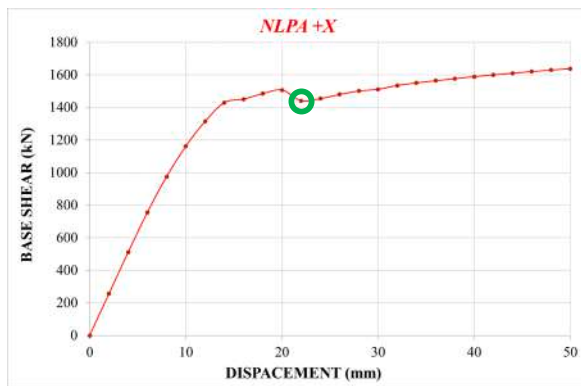
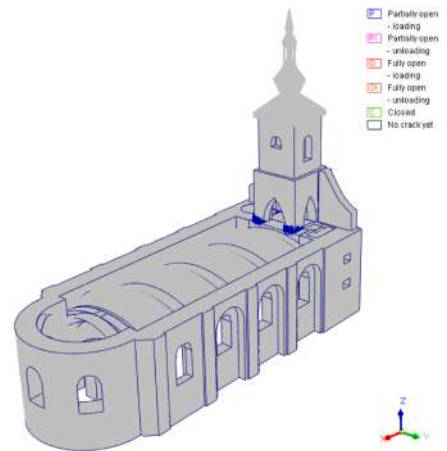
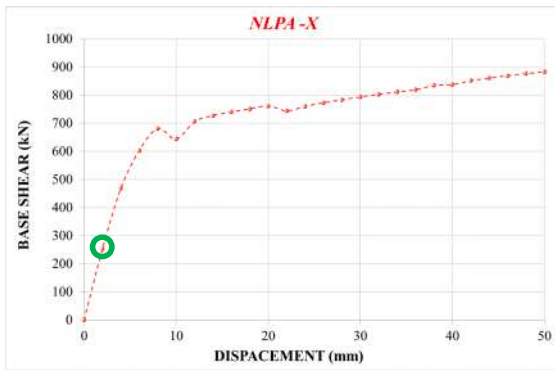
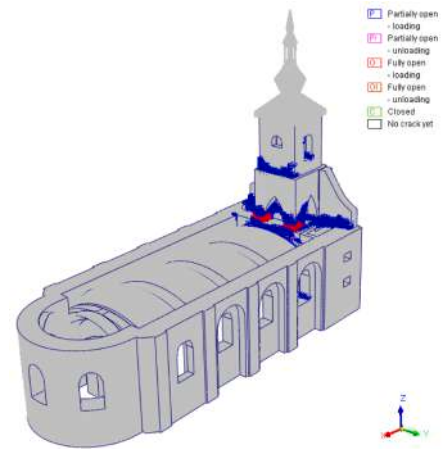
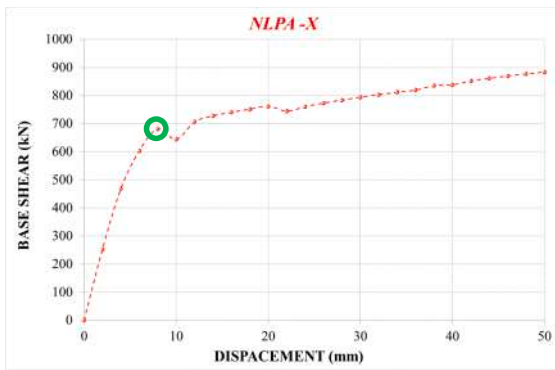


Fig. 14. *NLPA+X*: capacity curve and crack status for several load steps increments.

1st LOAD INCREMENT – NLPA-X



4th LOAD INCREMENT – NLPA-X



5th LOAD INCREMENT – NLPA-X

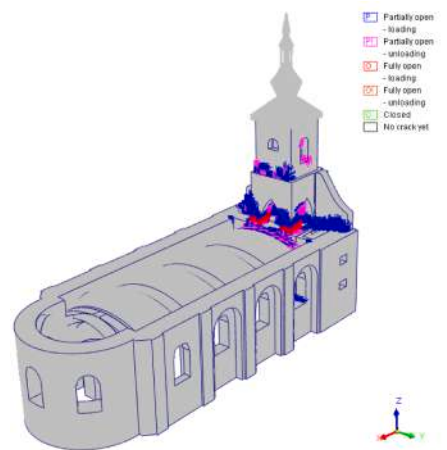
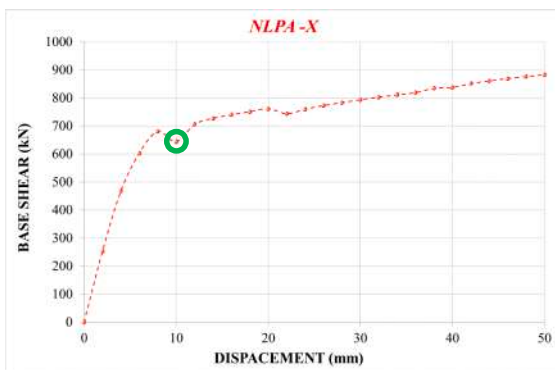


Fig. 15. NLPA-X: capacity curve and crack status for several load steps increments.

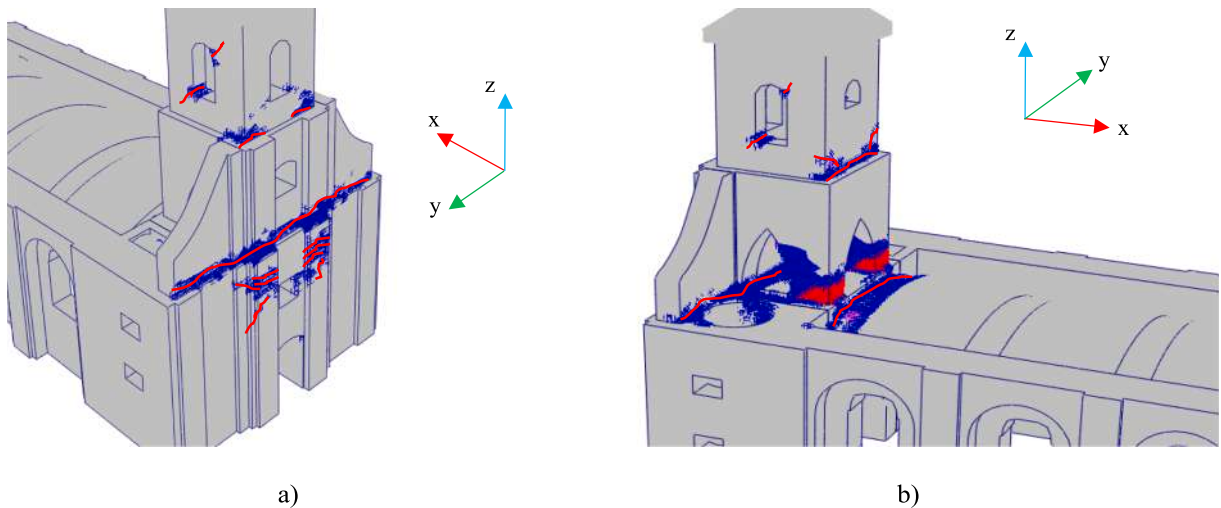


Fig. 16. Detail of the bell tower crack status: a) *NLPA+X*, third load step; b) *NLPA-X*, fourth load step.

In this study the results of four *NLPAs* are shown, that are two along the *X* direction (longitudinal direction, namely push *NLPA+X* and *NLPA-X*), and two along the *Y* direction (transverse direction, *NLPA+Y* and *NLPA-Y*). In each analysis, gravity loads are applied at first, and kept constant under an increasing lateral load simulating the horizontal seismic action. In this way a prediction of the seismic behaviour and of the seismic damage is obtained [10,39,58].

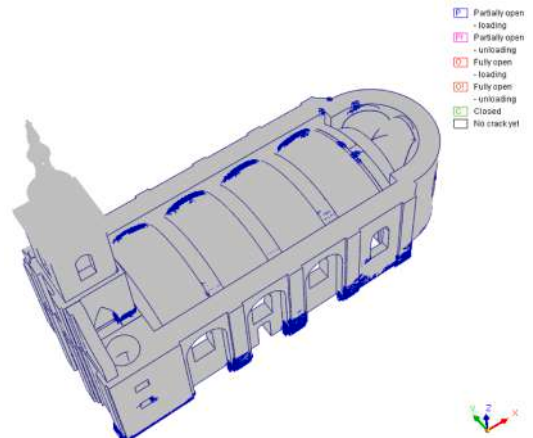
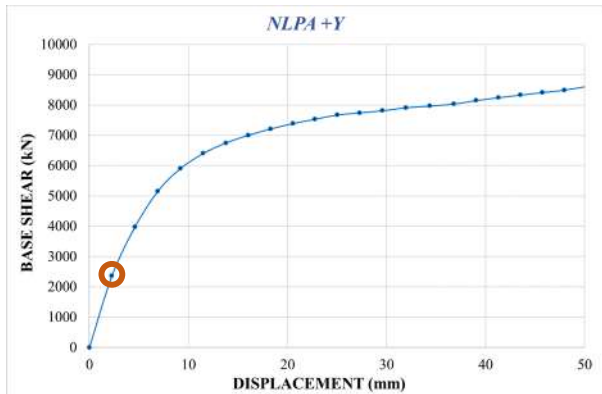
Fig. 14 through Fig. 18 report the results of the *NLPAs* performed. In particular, each figure shows the capacity curve (in the form of base shear vs displacement, the latter referred to the control node choice in all the analyses corresponding to the upper masonry portion of the belfry, at a height of 17 m, centrally on the side facing the nave), and a crack status for three load steps highlighted on the capacity curve.

In particular, as one may note as for *NLPA+X* (Fig. 14) localized horizontal cracks, due to an overturning, occur at base of the soaring portion of the bell tower and of the belfry. The same conclusion may be drawn in the case of *NLPA-X* (Fig. 15). The *NLPA+X* reaches higher values of base shear than the *NLPA-X* since, as it is possible to note, along this direction the aula vaulted structure is compressed while, in the case of the *NLPA-X*, it is in tension offering, on the contrary, a lower strength when the tower is pushed along the direction *-Y*. Both *NLPA+X* and *NLPA-X* highlights that along the longitudinal direction arises the overturning of the bell tower soaring portion, that is the most church vulnerable portion. Therefore, this conclusion validates the assumption of having this part as macro-element in the *LV2* approach. For completeness, Fig. 16a and Fig. 16b depict a detail of crack status onset where the bell tower damage is localized, referred respectively to the *NLPA+X* third load step and *NLPA-X* fourth load step of the *NLPAs*.

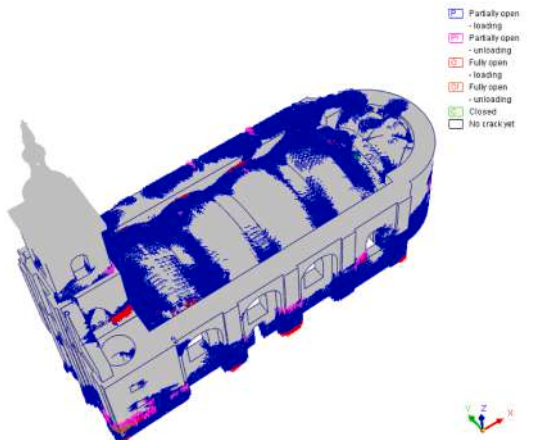
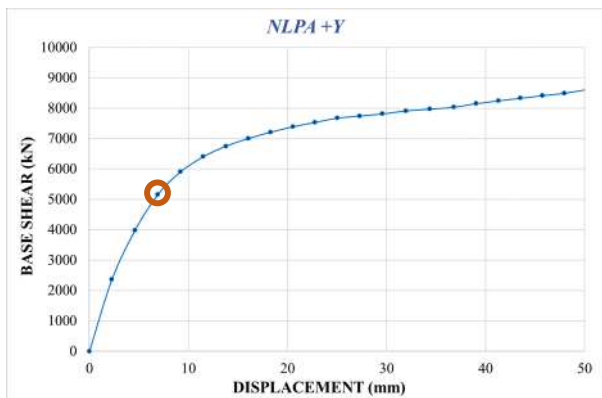
As regards the *NLPAs* performed along the transverse direction (*Y* direction), the results obtained are plotted in Fig. 17 and Fig. 18 for *NLPA+Y* and *NLPA-Y*, respectively. In this case, differently for the *NLPAs* along the *X* direction, cracks are not localized in a specific portion of the church, but they are widespread in all the masonry elements, such as walls, aula arches, triumphal arch, barrel vaults, bell tower, and apse. Moreover, cracks distributions are quite similar for both *NLPA+Y* (Fig. 17) and *NLPA-Y* (Fig. 18). Therefore, in this case it is not possible to identify a unique local mechanism (such as the bell tower in the case of *NLPA+X/NLPA-X*), but all the architectural portions (i.e. macro-elements) interact among them in the global response. Fig. 19 reports a particular of the crack status referred to the second step of the push-over analyses. Of course, this result is deeply conditioned by constructions details knowledge (such connection degree among the elements, presence of interventions, and of current crack patterns) that, as known, heavily influence the numerical modelling. They are essential in defining numerical models and in identifying the potential local response mechanisms that may occur. In the case analysed all the elements are assumed to be perfectly collaborating each other by ignoring, therefore, any local situation that may modify the assumption made. Therefore, the assumption made with the *LV2* method with respect to the lateral response tends to overestimate the church current capacity since, due to the interaction among the elements, a premature failure may occur in lateral walls before the aula arches collapse.

Finally, for sake of completeness, Fig. 20 plots a comparison among the four pushover curves obtained (such as *NLPA+X*, *NLPA-X*, *NLPA+Y* and *NLPA-Y*). One may easily note that *NLPA+Y* and *NLPA-Y* (along the transverse direction) are quite similar providing higher curves with respect to *NLPA+X* and *NLPA-X*. This is due to the fact that, as already discussed, under the assumption made along the *Y* direction a global response is obtained, contrarily to the *X* direction, where a clear local response is observed given by the bell tower overturning.

1st LOAD INCREMENT – *NLPA+Y*



3rd LOAD INCREMENT – *NLPA+Y*



8th LOAD INCREMENT – *NLPA+Y*

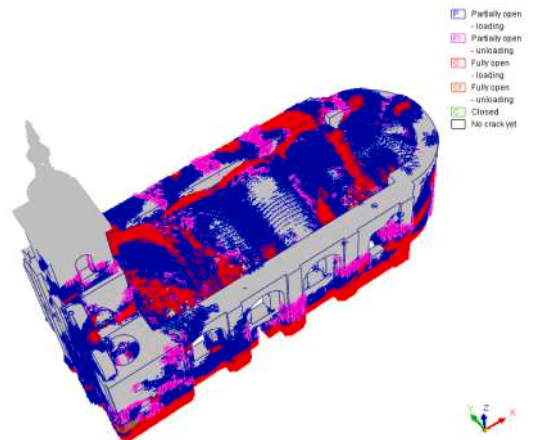
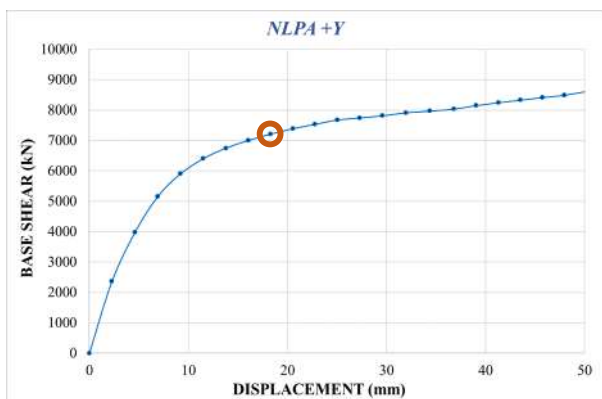
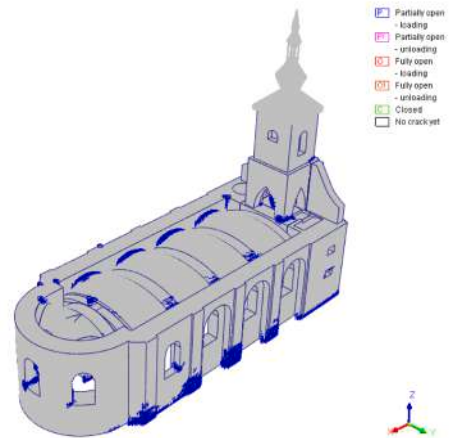
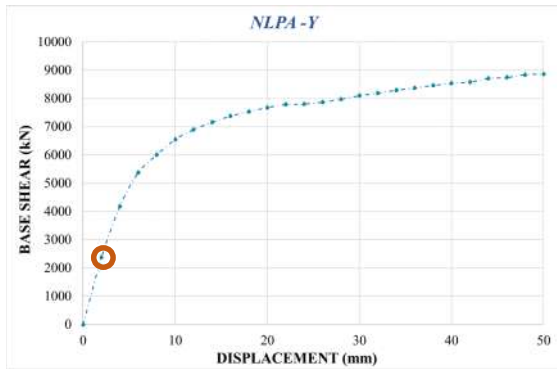
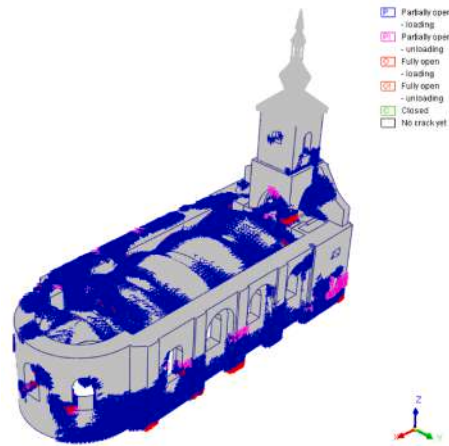
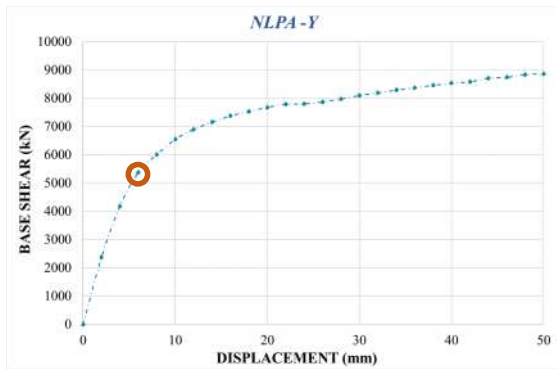


Fig. 17. *NLPA+Y*: capacity curve and crack status for several load steps increments.

1st LOAD INCREMENT – *NLPA-Y*



3rd LOAD INCREMENT – *NLPA-Y*



9th LOAD INCREMENT – *NLPA-Y*

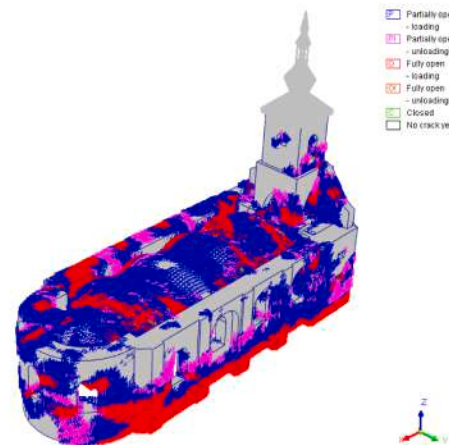
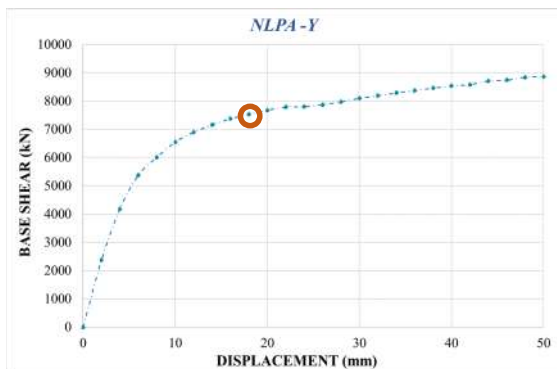


Fig. 18. *NLPA-Y*: capacity curve and crack status for several load steps increments.

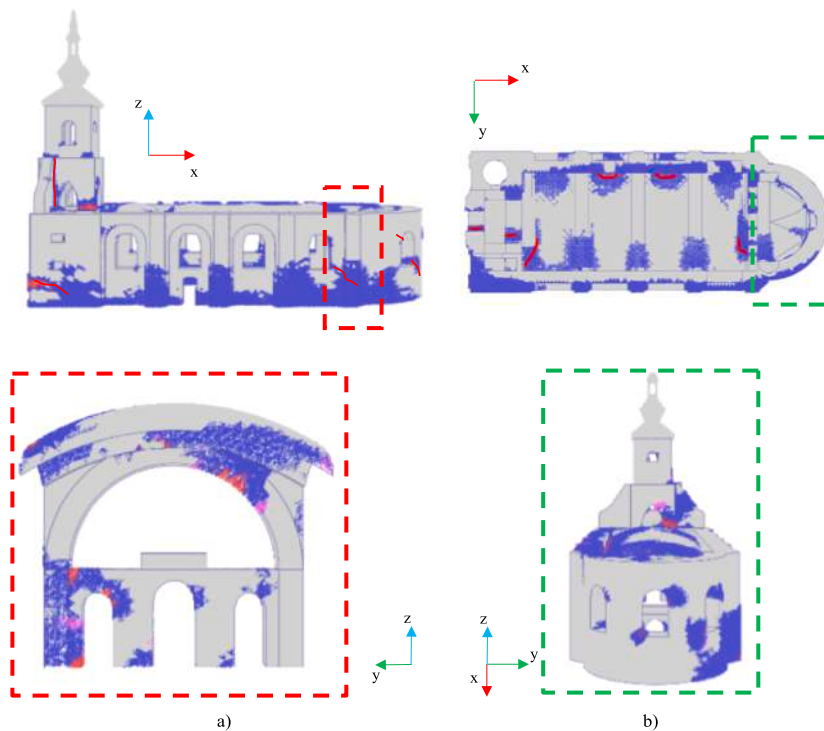


Fig. 19. Crack status: a) NLPA+Y, second load step; b) NLPA-Y, second load step.

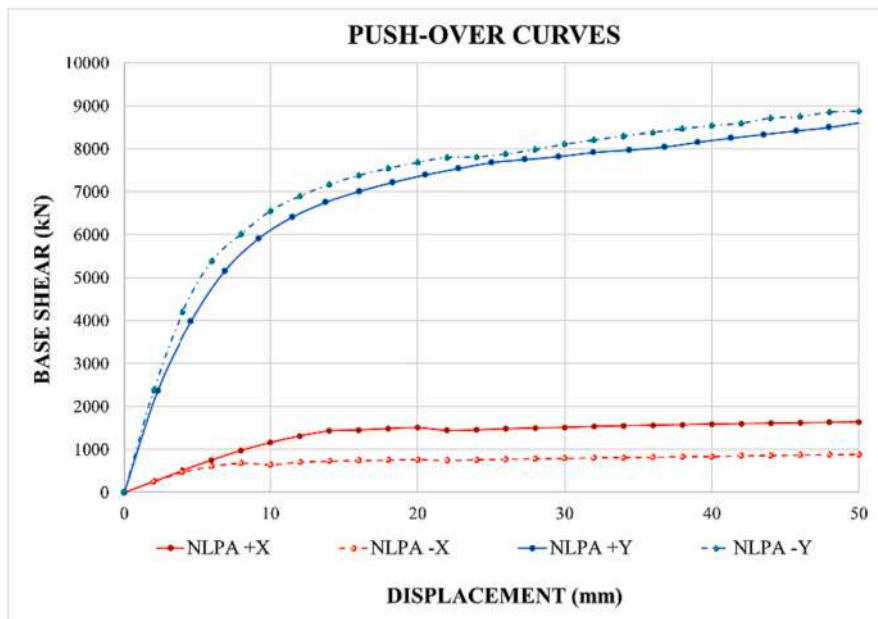


Fig. 20. Comparison among the non-linear pushover curves obtained.

5. Concluding remarks

In this paper, the seismic assessment of Romanian Orthodox masonry churches, through a multi-level approach, has been presented. To this purpose the Italian multi-level approach has been used, proposed for Italian churches and extended in the case of Romanian churches for evaluations at a different scale level. First of all, allows to screen rapidly the sample of case studies investigated at a territorial level. By means of only qualitative information, a ranking of the obtained results may be obtained in order to identify

priorities and to plan further and more refined investigations. Therefore, this Level of Valuation (named *LV0* and *LV1*) is without any doubt a convenient tool to preliminary assess situations requiring particular attention and deeper investigations. Then, local analyses through the *LV2* approach, and global *LV3* analyses implying a FEM models may be applied in order to assess the seismic performance and to design possible interventions.

As first step, in this study a territorial evaluation (*LV0* and *LV1*) has been conducted on a sample of six churches located in the Banat region. Afterwards, one church representative of the case studies sample considered has been analysed through more refined local and global analyses. In particular, local kinematic limit analysis (as for the *LV2*) and global non-linear push-over analysis (*LV3*) have been conducted. The former has been utilized for evaluating activation thresholds of the potential response mechanisms of some principal architectural parts (such as, aula arches, façade, bell tower). Whereas, the latter has been useful for identifying, by means of crack status obtained, the most vulnerable response mechanism, corresponding in this case with the soaring portion of the bell tower. Moreover, *LV3* approach has clearly demonstrated that along the transverse response (Y direction) all the architectural portions (i.e. macro-elements) interact among them in the global response. Therefore, the knowledge of the construction details (such connection degree among the elements, presence of interventions, and of current crack patterns) is essential to correctly implement the FEM model for numerical simulations.

Finally, in the cases analysed the multi-level approach has demonstrated that the simplified global *LV1* is only a fast tool for comparing at a territorial level several churches but, anyway, local analyses have to be carried out in order to identify the most vulnerable mechanisms, which may vary case-by-case depending on local conditions found.

In future additional numerical elaborations will be conducted on the other churches of the sample considered. In particular, they will be also addressed to study the effects of the vertical seismic component that, as known, is not negligible in the case of shallow earthquakes typically affecting in the Banat region, for which specific recommendations in the Romanian national code are still lacking.

Declaration of Competing Interest

The authors declare that they have no known competing financial interests or personal relationships that could have appeared to influence the work reported in this paper.

Data availability

The authors are unable or have chosen not to specify which data has been used.

Appendix A

Table 6

LV0: hazard and vulnerability calculation on Holy Spirit Descent Church (Biserică Pogorărea Sfântului Duh) – Cenad.

Cenad church <i>H</i> = 0.46		Severity of the damage $h_{k,j}$ (hazard)			Cenad church <i>V</i> = 40.41	Vulnerability $v_{k,j}$				Weight	
Threats		No damage/ no hazard	Low or gradual	Catastrophic	Parameters	A	B	C	D	ρ_k	TOT
Sporadic events	Seismic action	0.00	<u>0.20</u>	0.40	Position of the building and foundations	<u>0.00</u>	1.35	6.73	12.12	0.75	0.00
	Landslides or faults	<u>0.00</u>	0.15	0.25	Floor plan configuration or geometry	0.00	1.35	<u>6.73</u>	12.12	0.50	3.37
	Volcanic threat	<u>0.00</u>	0.20	0.40	Elevation configuration	0.00	1.35	6.73	<u>12.12</u>	1.00	12.12
	Hydro-meteorological threat	0.00	<u>0.15</u>	0.25	Distance between walls	0.00	<u>1.35</u>	6.73	12.12	0.25	0.34
	Chemical-technological threat	<u>0.00</u>	0.15	0.25	Non-structural elements	0.00	<u>1.35</u>	6.73	12.12	0.25	0.34
	Forest fires	<u>0.00</u>	0.15	0.25	Type and organisation of the resistant system	0.00	<u>1.35</u>	6.73	12.12	1.50	2.03
Continuous processes	Erosion (precipitation)	0.00	<u>0.05</u>	0.1	Quality of the resistant system	0.00	<u>1.35</u>	6.73	12.12	0.25	0.34
	Physical stress (temperature fluctuations)	0.00	<u>0.05</u>	0.1	Horizontal structures	0.00	1.35	6.73	<u>12.12</u>	1.00	12.12
	Air pollution	<u>0.00</u>	0.01	0.05	Roofing configuration	0.00	<u>1.35</u>	6.73	12.12	1.00	1.35
	Socio-organisational (excessive tourism, potential vandalism)	<u>0.00</u>	0.01	0.05	Conservation status	0.00	1.35	<u>6.73</u>	12.12	1.00	6.73
	Demographic decline (abandonment)	0.00	<u>0.01</u>	0.05	Environmental alterations	<u>0.00</u>	1.35	6.73	12.12	0.25	0.00
					Construction system alterations	<u>0.00</u>	1.35	6.73	12.12	0.25	0.00
					Fire vulnerability	0.00	1.35	<u>6.73</u>	12.12	0.25	1.68

Table 7

LVO: hazard and vulnerability calculation on Virgin Mary's Nativity Church (Biserică Nașterea Maicii Domnului) - Chizătău.

Chizătău church		Severity of the damage $h_{k,j}$ (hazard)			Chizătău church	Vulnerability $v_{k,j}$				Weight	
$H = 0.56$					$V = 37.37$						
Threats		No damage/ no hazard	Low or gradual	Catastrophic	parameters	A	B	C	D	ρ_k	TOT
Sporadic events	Seismic action	0.00	<u>0.20</u>	0.40	Position of the building and foundations	<u>0.00</u>	1.35	6.73	12.12	0.75	0.00
	Landslides or faults	<u>0.00</u>	0.15	0.25	Floor plan configuration or geometry	0.00	1.35	6.73	<u>12.12</u>	0.50	6.06
	Volcanic threat	<u>0.00</u>	0.20	0.40	Elevation configuration	0.00	1.35	6.73	<u>12.12</u>	1.00	12.12
	Hydro-meteorological threat	0.00	<u>0.15</u>	0.25	Distance between walls	<u>0.00</u>	1.35	6.73	12.12	0.25	0.00
	Chemical-technological threat	<u>0.00</u>	0.15	0.25	Non-structural elements	0.00	<u>1.35</u>	6.73	12.12	0.25	0.34
	Forest fires	0.00	<u>0.15</u>	0.25	Type and organisation of the resistant system	0.00	<u>1.35</u>	6.73	12.12	1.5	2.03
Continuous processes	Erosion (precipitation)	0.00	<u>0.05</u>	0.10	Quality of the resistant system	0.00	<u>1.35</u>	6.73	12.12	0.25	0.34
	Physical stress (temperature fluctuations)	<u>0.00</u>	0.05	0.10	Horizontal structures	0.00	1.35	<u>6.73</u>	12.12	1.00	6.73
	Air pollution	<u>0.00</u>	0.01	0.05	Roofing configuration	0.00	<u>1.35</u>	6.73	12.12	1	1.35
	Socio-organisational (excessive tourism, potential vandalism)	<u>0.00</u>	0.01	0.05	Conservation status	0.00	1.35	<u>6.73</u>	12.12	1.00	6.73
	Demographic decline (abandonment)	0.00	<u>0.01</u>	0.05	Environmental alterations	<u>0.00</u>	1.35	6.73	12.12	0.25	0.00
					Construction system alterations	<u>0.00</u>	1.35	6.73	12.12	0.25	0.00
					Fire vulnerability	0.00	1.35	<u>6.73</u>	12.12	0.25	1.68

Table 8

LVO: hazard and vulnerability calculation on Saint Nicholas Church (Biserică Sfântul Nicolae) - Bocșa.

Bocșa church		Severity of the damage $h_{k,j}$ (hazard)			Bocșa church	Vulnerability $v_{k,j}$				Weight	
$H = 0.73$					$V = 29.63$						
Threats		No damage/ no hazard	Low or gradual	Catastrophic	parameters	A	B	C	D	ρ_k	TOT
Sporadic events	Seismic action	0.00	<u>0.20</u>	0.40	Position of the building and foundations	<u>0.00</u>	1.35	6.73	12.12	0.75	0.00
	Landslides or faults	0.00	<u>0.15</u>	0.25	Floor plan configuration or geometry	0.00	1.35	<u>6.73</u>	12.12	0.50	3.37
	Volcanic threat	<u>0.00</u>	0.20	0.40	Elevation configuration	0.00	1.35	6.73	<u>12.12</u>	1.00	12.12
	Hydro-meteorological threat	0.00	<u>0.15</u>	0.25	Distance between walls	<u>0.00</u>	1.35	6.73	12.12	0.25	0.00
	Chemical-technological threat	<u>0.00</u>	0.15	0.25	Non-structural elements	0.00	<u>1.35</u>	6.73	12.12	0.25	0.34
	Forest fires	0.00	<u>0.15</u>	0.25	Type and organisation of the resistant system	0.00	<u>1.35</u>	6.73	12.12	1.50	2.03
Continuous processes	Erosion (precipitation)	0.00	<u>0.05</u>	0.10	Quality of the resistant system	0.00	1.35	<u>6.73</u>	12.12	0.25	1.68
	Physical stress (temperature fluctuations)	<u>0.00</u>	0.05	0.10	Horizontal structures	0.00	1.35	<u>6.73</u>	12.12	1	6.73
	Air pollution	0.00	<u>0.01</u>	0.05	Roofing configuration	0.00	<u>1.35</u>	6.73	12.12	1	1.35
	Socio-organisational (excessive tourism, potential vandalism)	0.00	<u>0.01</u>	0.05	Conservation status	<u>0.00</u>	1.35	6.73	12.12	1.00	0.00
	Demographic decline (abandonment)	0.00	<u>0.01</u>	0.05	Environmental alterations	<u>0.00</u>	1.35	6.73	12.12	0.25	0.00
					Construction system alterations	0.00	<u>1.35</u>	6.73	12.12	0.25	0.34
					Fire vulnerability	0.00	1.35	<u>6.73</u>	12.12	0.25	1.68

Table 9

LVO: hazard and vulnerability calculation on Saint Nicholas Church (Biserică Sfântul Nicolae) - Bencecu de Jos.

Bencecu de Jos church <i>H</i> = 0.46		Severity of the damage $h_{k,j}$ (hazard)			Bencecu de Jos church <i>V</i> = 34.68	Vulnerability $v_{k,j}$				Weight	
Threats		No damage/ no hazard	Low or gradual	Catastrophic	parameters	A	B	C	D	ρ_k	TOT
Sporadic events	Seismic action	0.00	<u>0.20</u>	0.40	Position of the building and foundations	<u>0.00</u>	1.35	6.73	12.12	0.75	0.00
	Landslides or faults	0.00	<u>0.15</u>	0.25	Floor plan configuration or geometry	0.00	1.35	6.73	<u>12.12</u>	0.50	6.06
	Volcanic threat	<u>0.00</u>	0.20	0.40	Elevation configuration	0.00	1.35	6.73	<u>12.12</u>	1.00	12.12
	Hydro-meteorological threat	<u>0.00</u>	0.15	0.25	Distance between walls	0.00	<u>1.35</u>	6.73	12.12	0.25	0.34
	Chemical-technological threat	<u>0.00</u>	0.15	0.25	Non-structural elements	0.00	<u>1.35</u>	6.73	12.12	0.25	0.34
	Forest fires	<u>0.00</u>	0.15	0.25	Type and organisation of the resistant system	0.00	<u>1.35</u>	6.73	12.12	1.50	2.03
Continuous processes	Erosion (precipitation)	0.00	<u>0.05</u>	0.10	Quality of the resistant system	<u>0.00</u>	1.35	6.73	12.12	0.25	0.00
	Physical stress (temperature fluctuations)	0.00	<u>0.05</u>	0.10	Horizontal structures	0.00	1.35	6.73	<u>12.12</u>	1.00	12.12
	Air pollution	<u>0.00</u>	0.01	0.05	Roofing configuration	<u>0.00</u>	1.35	6.73	12.12	1.00	0.00
	Socio-organisational (excessive tourism, potential vandalism)	<u>0.00</u>	0.01	0.05	Conservation status	<u>0.00</u>	1.35	6.73	12.12	1.00	0.00
	Demographic decline (abandonment)	0.00	<u>0.01</u>	0.05	Environmental alterations	<u>0.00</u>	1.35	6.73	12.12	0.25	0.00
					Construction system alterations	<u>0.00</u>	1.35	6.73	12.12	0.25	0
					Fire vulnerability	0.00	1.35	<u>6.73</u>	12.12	0.25	1.68

Table 10

LVO: hazard and vulnerability calculation on Saint George Church (Biserică Sfântul Gheorghe) - Beregsău Mare.

Beregsău Mare church <i>H</i> = 0.46		Severity of the damage $h_{k,j}$ (hazard)			Beregsău Mare church <i>V</i> = 32.66	Vulnerability $v_{k,j}$				Weight	
Threats		No damage/ no hazard	Low or gradual	Catastrophic	parameters	A	B	C	D	ρ_k	TOT
Sporadic events	Seismic action	0.00	<u>0.20</u>	0.40	Position of the building and foundations	<u>0.00</u>	1.35	6.73	12.12	0.75	0
	Landslides or faults	<u>0.00</u>	0.15	0.25	Floor plan configuration or geometry	0.00	1.35	<u>6.73</u>	12.12	0.5	3.37
	Volcanic threat	<u>0.00</u>	0.20	0.40	Elevation configuration	0.00	1.35	6.73	<u>12.12</u>	1.00	12.12
	Hydro-meteorological threat	0.00	<u>0.15</u>	0.25	Distance between walls	0.00	<u>1.35</u>	6.73	12.12	0.25	0.34
	Chemical-technological threat	<u>0.00</u>	0.15	0.25	Non-structural elements	0.00	<u>1.35</u>	6.73	12.12	0.25	0.34
	Forest fires	<u>0.00</u>	0.15	0.25	Type and organisation of the resistant system	<u>0.00</u>	1.35	6.73	12.12	1.5	0.00
Continuous processes	Erosion (precipitation)	0.00	<u>0.05</u>	0.10	Quality of the resistant system	<u>0.00</u>	1.35	6.73	12.12	0.25	0.00
	Physical stress (temperature fluctuations)	0.00	<u>0.05</u>	0.10	Horizontal structures	0.00	<u>1.35</u>	6.73	12.12	1.00	1.35
	Air pollution	<u>0.00</u>	0.01	0.05	Roofing configuration	0.00	<u>1.35</u>	6.73	12.12	1.00	1.35
	Socio-organisational (excessive tourism, potential vandalism)	<u>0.00</u>	0.01	0.05	Conservation status	0.00	1.35	6.73	<u>12.12</u>	1.00	12.12
	Demographic decline (abandonment)	0.00	<u>0.01</u>	0.05	Environmental alterations	<u>0.00</u>	1.35	6.73	12.12	0.25	0.00
					Construction system alterations	<u>0.00</u>	1.35	6.73	12.12	0.25	0.00
					Fire vulnerability	0.00	1.35	<u>6.73</u>	12.12	0.25	1.68

Table 11

LVO: hazard and vulnerability calculation on Jesus Resurrection Church (Biserică Învierea Domnului) – Belinț.

Belinț church <i>H</i> = 0.41		Severity of the damage $h_{k,j}$ (hazard)			Belinț church <i>V</i> = 30.98	Vulnerability $v_{k,j}$				Weight	
Threats		No damage/ no hazard	Low or gradual	Catastrophic	parameters	A	B	C	D	ρ_k	TOT
Sporadic events	Seismic action	0.00	<u>0.20</u>	0.40	Position of the building and foundations	<u>0.00</u>	1.35	6.73	12.12	0.75	0.00
	Landslides or faults	<u>0.00</u>	0.15	0.25	Floor plan configuration or geometry	0.00	1.35	6.73	<u>12.12</u>	0.50	6.06
	Volcanic threat	<u>0.00</u>	0.20	0.40	Elevation configuration	0.00	1.35	6.73	<u>12.12</u>	1.00	12.12
	Hydro-meteorological threat	<u>0.00</u>	0.15	0.25	Distance between walls	0.00	<u>1.35</u>	6.73	12.12	0.25	0.34
	Chemical-technological threat	<u>0.00</u>	0.15	0.25	Non-structural elements	0.00	<u>1.35</u>	6.73	12.12	0.25	0.34
	Forest fires	0.00	<u>0.15</u>	0.25	Type and organisation of the resistant system	0.00	<u>1.35</u>	6.73	12.12	1.5	2.03
Continuous processes	Erosion (precipitation)	0.00	<u>0.05</u>	0.10	Quality of the resistant system	<u>0.00</u>	1.35	6.73	12.12	0.25	0.00
	Physical stress (temperature fluctuations)	<u>0.00</u>	0.05	0.10	Horizontal structures	0.00	1.35	<u>6.73</u>	12.12	1.00	6.73
	Air pollution	<u>0.00</u>	0.01	0.05	Roofing configuration	0.00	<u>1.35</u>	6.73	12.12	1.00	1.35
	Socio-organisational (excessive tourism, potential vandalism)	<u>0.00</u>	0.01	0.05	Conservation status	<u>0.00</u>	1.35	6.73	12.12	1.00	0.00
	Demographic decline (abandonment)	0.00	<u>0.01</u>	0.05	Environmental alterations	<u>0.00</u>	1.35	6.73	12.12	0.25	0.00
					Construction system alterations	0.00	<u>1.35</u>	6.73	12.12	0.25	0.34
					Fire vulnerability	0.00	1.35	<u>6.73</u>	12.12	0.25	1.68

Appendix B

Table 12

LVI: vulnerability parameters calculation on Holy Spirit Descent Church (Biserică Pogorârea Sfântului Duh) in Cenad and on Virgin Mary’s Nativity Church (Biserică Nașterea Maicii Domnului) in Chizătău.

Cenad church				Chizătău church			
Elements	ρ_k	v_{ki}	v_{kp}	Elements	ρ_k	v_{ki}	v_{kp}
overturning of the facade	1	0	1	overturning of the facade	1	0	3
mechanisms in the top of the facade	1	0	0	mechanisms in the top of the facade	0	0	0
plane mechanisms of the facade	1	2	0	plane mechanisms of the facade	0	0	0
prothyrum - narthex	0.5	0	2	prothyrum - narthex	0	0	0
transversal response of the nave	1	1	1	transversal response of the nave	1	2	3
shear mechanisms in the side walls	1	1	0	shear mechanisms in the side walls	1	1	2
colonnade longitudinal response	0	0	0	colonnade longitudinal response	0	0	0
central nave vaults	1	2	0	central nave vaults	1	3	0
vaults in the aisles	0	0	0	vaults in the aisles	0	0	0
overturning of the end of transept walls	0.9	1	2	overturning of the end of transept walls	0	0	0
shear mechanisms on the transept walls	0.9	1	0	shear mechanisms on the transept walls	0	0	0
transept vaults	0.8	2	0	transept vaults	0	0	0
triumphal arches	0	0	0	triumphal arches	0	0	0
dome-tiburium	0	0	0	dome-tiburium	0	0	0
church lantern	0	0	0	church lantern	0	0	0
apse overturning,	1	2	2	apse overturning,	1	2	0
shear mechanisms in the presbytery/apse	1	1	0	shear mechanisms in the presbytery/apse	1	2	2
presbytery or apse vaults	0.9	2	0	presbytery or apse vaults	0.7	3	0
roof elements mechanisms: side walls of the hall	1	0	0	roof elements mechanisms: side walls of the hall	0.5	1	0
roof elements mechanisms: transept	0.8	0	0	roof elements mechanisms: transept	0	0	0
roof elements mechanisms: apse and presbytery	1	0	0	roof elements mechanisms: apse and presbytery	0.5	1	0
chapels overturning	0	0	0	chapels overturning	0	0	0
shear mechanisms on the walls of the chapels	0	0	0	shear mechanisms on the walls of the chapels	0	0	0
chapels vaults	0	0	0	chapels vaults	0	0	0
interactions near to plane-altimetric irregularities	0	0	0	interactions near to plane-altimetric irregularities	0	0	0
overhangs (spires, pinnacles, statues)	0.7	1	0	overhangs (spires, pinnacles, statues)	0.6	1	2
bell tower	1	3	1	bell tower	1	3	2
belfry	1	0	1	belfry	0	0	0

Table 13

LVI: vulnerability parameters calculation on Saint Nicholas Church (Biserică Sfântul Nicolae) in Bocșa and on Saint Nicholas Church (Biserică Sfântul Nicolae) in Bencecu de Jos churches.

Bocșa church				Bencecu de Jos church			
Elements	ρ_k	ν_{ki}	ν_{kp}	Elements	ρ_k	ν_{ki}	ν_{kp}
overturning of the facade	1	0	1	overturning of the facade	1	0	2
mechanisms in the top of the facade	1	0	0	mechanisms in the top of the facade	1	0	0
plane mechanisms of the facade	1	0	0	plane mechanisms of the facade	1	0	0
prothyrum - narthex	0	0	0	prothyrum - narthex	0	0	0
transversal response of the nave	1	3	3	transversal response of the nave	1	1	2
shear mechanisms in the side walls	1	0	2	shear mechanisms in the side walls	1	2	2
colonnade longitudinal response	0	0	0	colonnade longitudinal response	0	0	0
central nave vaults	1	1	2	central nave vaults	1	3	1
vaults in the aisles	0	0	0	vaults in the aisles	0	0	0
overturning of the end of transept walls	0	0	0	overturning of the end of transept walls	0.9	1	2
shear mechanisms on the transept walls	0	0	0	shear mechanisms on the transept walls	0.9	1	2
transept vaults	0	0	0	transept vaults	0.8	1	0
triumphal arches	1	0	1	triumphal arches	1	0	1
dome-tiburium	0	0	0	dome-tiburium	0	0	0
church lantern	0	0	0	church lantern	0	0	0
apse overturning,	1	1	0	apse overturning,	1	0	1
shear mechanisms in the presbytery/apse	1	0	2	shear mechanisms in the presbytery/apse	1	1	2
presbytery or apse vaults	0.9	1	0	presbytery or apse vaults	0.9	1	0
roof elements mechanisms: side walls of the hall	1	0	0	roof elements mechanisms: side walls of the hall	1	0	0
roof elements mechanisms: transept	0	0	0	roof elements mechanisms: transept	0.8	0	0
roof elements mechanisms: apse and presbytery	1	0	0	roof elements mechanisms: apse and presbytery	1	0	0
chapels overturning	0	0	0	chapels overturning	0	0	0
shear mechanisms on the walls of the chapels	0	0	0	shear mechanisms on the walls of the chapels	0	0	0
chapels vaults	0	0	0	chapels vaults	0	0	0
interactions near to plane-altimetric irregularities	0	0	0	interactions near to plane-altimetric irregularities	0	0	0
overhangs (spires, pinnacles, statues)	0.8	2	0	overhangs (spires, pinnacles, statues)	0.7	1	0
bell tower	1	3	2	bell tower	1	1	2
belfry	1	0	1	belfry	1	0	1

Table 14

LVI: vulnerability parameters calculation on Saint George Church (Biserică Sfântul Gheorghe) in Beregsău Mare and on Jesus Resurrection Church (Biserică Învierea Domnului) in Belinț churches.

Beregsău Mare church				Belinț church			
Elements	ρ_k	ν_{ki}	ν_{kp}	Elements	ρ_k	ν_{ki}	ν_{kp}
overturning of the facade	1	1	2	overturning of the facade	1	0	3
mechanisms in the top of the facade	1	0	0	mechanisms in the top of the facade	0	0	0
plane mechanisms of the facade	1	0	0	plane mechanisms of the facade	0	0	0
prothyrum - narthex	0.5	0	2	prothyrum - narthex	0	0	0
transversal response of the nave	1	2	0	transversal response of the nave	1	2	3
shear mechanisms in the side walls	1	0	2	shear mechanisms in the side walls	1	2	2
colonnade longitudinal response	0	0	0	colonnade longitudinal response	0	0	0
central nave vaults	1	0	3	central nave vaults	1	0	1
vaults in the aisles	0	0	0	vaults in the aisles	0	0	0
overturning of the end of transept walls	0	0	0	overturning of the end of transept walls	0	0	0
shear mechanisms on the transept walls	0	0	0	shear mechanisms on the transept walls	0	0	0
transept vaults	0	0	0	transept vaults	0	0	0
triumphal arches	1	0	0	triumphal arches	1	0	1
dome-tiburium	0	0	0	dome-tiburium	0	0	0
church lantern	0	0	0	church lantern	0	0	0
apse overturning,	1	2	0	apse overturning,	1	3	0
shear mechanisms in the presbytery/apse	1	0	2	shear mechanisms in the presbytery/apse	1	2	2
presbytery or apse vaults	0.9	0	0	presbytery or apse vaults	0.9	0	1
roof elements mechanisms: side walls of the hall	1	0	0	roof elements mechanisms: side walls of the hall	1	0	2
roof elements mechanisms: transept	0	0	0	roof elements mechanisms: transept	0	0	0
roof elements mechanisms: apse and presbytery	1	0	0	roof elements mechanisms: apse and presbytery	1	0	2
chapels overturning	0	0	0	chapels overturning	0	0	0
shear mechanisms on the walls of the chapels	0	0	0	shear mechanisms on the walls of the chapels	0	0	0
chapels vaults	0	0	0	chapels vaults	0	0	0
interactions near to plane-altimetric irregularities	0	0	0	interactions near to plane-altimetric irregularities	0	0	0
overhangs (spires, pinnacles, statues)	0.8	0	2	overhangs (spires, pinnacles, statues)	0.6	2	1
bell tower	1	3	2	bell tower	1	2	2
belfry	1	0	1	belfry	1	0	1

References

- [1] I. Apostol, Seismic Vulnerability Assessment of Historical Urban Centres (in Romanian), Polytechnic University of Timișoara, Timișoara, 2020. http://www.upt.ro/img/files/2019-2020/doctorat/teze/rezumate/Apostol_Jasmina_Rezumate_teza_engleza.pdf.
- [2] A. Bala, V. Raileanu, C. Dinu, M. Diaconescu, Crustal seismicity and active fault systems in Romania, Rom. Rep. Phys 67 (3) (2015) 1176–1191. https://www.researchgate.net/profile/Mihail-Diaconescu/publication/282150077_Crustal_seismicity_and_active_fault_systems_in_Romania/links/5605123f08aea25fce321134/Crustal-seismicity-and-active-fault-systems-in-Romania.pdf.
- [3] J. Batt, Reinventing Banat, Reg. Federal Studies 12 (2) (2002) 178–202, <https://doi.org/10.1080/714004738>.
- [4] P. Block, T. Ciblac, J. Ochsendorf, Real-time limit analysis of vaulted masonry buildings, Comput. Struct. 84 (29–30) (2006) 1841–1852, <https://doi.org/10.1016/j.compstruc.2006.08.002>.
- [5] P. de Buhán, G. de Felice, A homogenization approach to the ultimate strength of brick masonry, J. Mech. Phys. Solids 45 (7) (1997) 1085–1104, [https://doi.org/10.1016/S0022-5096\(97\)00002-1](https://doi.org/10.1016/S0022-5096(97)00002-1).
- [6] L. Cascini, R. Gagliardo, F. Portioli, LiABlock 3D: a software tool for collapse mechanism analysis of historic masonry structures, Int. J. Arch. Heritage 14 (1) (2020) 75–94, <https://doi.org/10.1080/15583058.2018.1509155>.
- [7] N. Chieffo, M. Moscarca, A. Formisano, P.B. Lourenço, G. Milani, The effect of ground motion vertical component on the seismic response of historical masonry buildings: the case study of the Banloc Castle in Romania, Eng. Struct. 249 (2021), 113346, <https://doi.org/10.1016/j.engstruct.2021.113346>.
- [8] A. Chiozzi, N. Grillanda, G. Milani, A. Tralli, UB-ALMANAC: an adaptive limit analysis NURBS-based program for the automatic assessment of partial failure mechanisms in masonry churches, Eng. Fail. Anal. 85 (2018) 201–220, <https://doi.org/10.1016/j.engfailanal.2017.11.013>.
- [9] Circular n.7, 21.01.2019 - G.U. n.35. 2019. Ministry of Infrastructure and Transport.
- [10] F. Clementi, Failure analysis of Apennine masonry churches severely damaged during the 2016 Central Italy seismic sequence, Buildings 11 (2) (2021) 58, <https://doi.org/10.3390/buildings11020058>.
- [11] Code CEB-FIP Model. 1990. Comité Euro-International Du Béton (CEB), 1993.
- [12] CSPFEA - Engineering Solutions. 2023. "Midax FEA NX v1.1.
- [13] M. D'Amato, R. Gigliotti, R. Laguardia, Comparative seismic assessment of ancient masonry churches, Front. Built Environ. 5 (2019) 56, <https://doi.org/10.3389/fbuil.2019.00056>.
- [14] M. D'Amato, M. Laterza, D.D. Fuentes, Simplified seismic analyses of ancient churches in Matera's landscape, Int. J. Arch. Heritage 14 (1) (2020) 119–138, <https://doi.org/10.1080/15583058.2018.1511000>.
- [15] M. D'Amato, R. Sulla, Investigations of masonry churches seismic performance with numerical models: application to a case study, Arch. Civil Mech. Eng. 21 (4) (2021) 161, <https://doi.org/10.1007/s43452-021-00312-5>.
- [16] L. Danciu, S. Nandan, C. Reyes, R. Basili, G. Weatherill, C. Beauval, A. Rovida et al., 2021. The 2020 Update of the European Seismic Hazard Model - ESHM20: Model Overview.
- [17] F. Doglioni, A. Moretti, V. Petrini, Churches and the Earthquake, 1994. Edited by LINT. Trieste (in Italian).
- [18] Eurocode 8. 2004. CEN. EN 1998-1—Eurocode 8: Design of Structures for Earthquake Resistance—Part 1: General Rules, Seismic Actions and Rules for Buildings, Brussels, Belgium, 2004.
- [19] F. Fabbrocino, G. Vaiano, A. Formisano, M. D'Amato, Large-scale seismic vulnerability and risk of masonry churches in seismic-prone areas: two territorial case studies, Front. Built Environ. 5 (2019) 102, <https://doi.org/10.3389/fbuil.2019.00102>.
- [20] FEMA, Primer for Design Professionals (FEMA 389). Department of Homeland Security Emergency Preparedness and Response Directorate, Washington D.C., 2004.
- [21] A. Formisano, A. Marzo, Simplified and refined methods for seismic vulnerability assessment and retrofitting of an Italian cultural heritage masonry building, Comput. Struct. 180 (2017) 13–26, <https://doi.org/10.1016/j.compstruc.2016.07.005>.
- [22] A. Formisano, G. Ciccone, A. Mele, Large scale seismic vulnerability and risk evaluation of a masonry churches sample in the historical centre of Naples, 090003 (2017), <https://doi.org/10.1063/1.5012360>.
- [23] D.D. Fuentes, Design of Risk Assessment Tools for the Conservation of Immoveable Cultural Heritage. Application in Two Case Studies in the Northern Chilean Andes (in Spanish). Publicaciones Digitales ENCRyM, 2016. <https://mediateca.inah.gob.mx/repositorio/islandora/object/libro%3A836>.
- [24] D.D. Fuentes, P.A. Julià, M. D'Amato, M. Laterza, Preliminary seismic damage assessment of Mexican churches after September 2017 earthquakes, Int. J. Arch. Heritage 15 (4) (2021) 505–525, <https://doi.org/10.1080/15583058.2019.1628323>.
- [25] N. Grillanda, A. Chiozzi, G. Milani, A. Tralli, Tilting plane tests for the ultimate shear capacity evaluation of perforated dry joint masonry panels. Part II: numerical analyses, Eng. Struct. 228 (2021), 111460, <https://doi.org/10.1016/j.engstruct.2020.111460>.
- [26] N. Grillanda, A. Chiozzi, G. Milani, A. Tralli, NURBS solid modeling for the three-dimensional limit analysis of curved rigid block structures, Comput. Methods Appl. Mech. Eng. 399 (2022), 115304, <https://doi.org/10.1016/j.cma.2022.115304>.
- [27] N. Grillanda, M. Valente, G. Milani, ANUB-aggregates: a fully automatic NURBS-based software for advanced local failure analyses of historical masonry aggregates, Bull. Earthq. Eng. 18 (8) (2020) 3935–3961, <https://doi.org/10.1007/s10518-020-00848-6>.
- [28] G.U. n. 47. 2011. Prime Minister.
- [29] J. Heyman, The stone skeleton, Int. J. Solids Struct. 2 (2) (1966) 249–279, [https://doi.org/10.1016/0020-7683\(66\)90018-7](https://doi.org/10.1016/0020-7683(66)90018-7).
- [30] L. Hofer, P. Zampieri, M.A. Zanini, F. Faleschini, C. Pellegrino, Seismic damage survey and empirical fragility curves for churches after the August 24, 2016 Central Italy earthquake, Soil Dyn. Earthq. Eng. 111 (2018) 98–109, <https://doi.org/10.1016/j.soildyn.2018.02.013>.
- [31] A. Iannuzzo, M. Angelillo, E. De Chiara, F. De Guglielmo, F. De Serio, F. Ribera, A. Gesualdo, Modelling the cracks produced by settlements in masonry structures, Meccanica 53 (7) (2018) 1857–1873, <https://doi.org/10.1007/s11012-017-0721-2>.
- [32] S. Lagomarsino, Damage assessment of churches after L'Aquila earthquake (2009), Bull. Earthq. Eng. 10 (1) (2012) 73–92, <https://doi.org/10.1007/s10518-011-9307-x>.
- [33] P. Laihonon, "Language Ideologies in The Romanian Banat". Analysis of Interviews and Academic Writings among the Hungarians and Germans, University of Jyväskylä, Jyväskylä, 2009. <https://jyx.jyu.fi/bitstream/handle/123456789/20324/9789513936082.pdf?sequence=1&isAllowed=y>.
- [34] N. Lantada, J. Irizarry, A.H. Barbat, X. Goula, A. Roca, T. Susagna, L.G. Pujades, Seismic hazard and risk scenarios for Barcelona, Spain, using the risk-UE vulnerability index method, Bull. Earthq. Eng. 8 (2) (2010) 201–229, <https://doi.org/10.1007/s10518-009-9148-z>.
- [35] P.B. Lourenço, J.A. Roque, Simplified indexes for the seismic vulnerability of ancient masonry buildings, Constr. Build. Mater. 20 (4) (2006) 200–208, <https://doi.org/10.1016/j.conbuildmat.2005.08.027>.
- [36] R.C.G. Menin, L.M. Trautwein, T.N. Bittencourt, Modelos de Fissuração Distribuída Em Vigas de Concreto Armado Pelo Método Dos Elementos Finitos, Revista IBRACON de Estruturas e Materiais 2 (2) (2009) 166–200, <https://doi.org/10.1590/S1983-41952009000200004>.
- [37] G. Milani, P.B. Lourenço, A. Tralli, Homogenised limit analysis of masonry walls, part I: failure surfaces, Comput. Struct. 84 (3–4) (2006) 166–180, <https://doi.org/10.1016/j.compstruc.2005.09.005>.
- [38] G. Milani, Lesson learned after the Emilia-Romagna, Italy, 20–29 May 2012 earthquakes: a limit analysis insight on three masonry churches, Eng. Fail. Anal. 34 (2013) 761–778, <https://doi.org/10.1016/j.engfailanal.2013.01.001>.
- [39] G. Milani, M. Valente, Comparative pushover and limit analyses on seven masonry churches damaged by the 2012 Emilia-Romagna (Italy) seismic events: possibilities of non-linear finite elements compared with pre-assigned failure mechanisms, Eng. Fail. Anal. 47 (2015) 129–161, <https://doi.org/10.1016/j.engfailanal.2014.09.016>.
- [40] MIT. 2019. G.U. n. 35. Instructions for the Application of the "Update of the 'Technical Standards for Construction', Issued by D.M. 17/ 01/2018." Ministry of Infrastructure and Transport.
- [41] A. Lo Monaco, N. Grillanda, I. Onescu, M. Fofiu, F. Clementi, M. D'Amato, A. Formisano, G. Milani, M. Moscarca, Seismic assessment of typical historical masonry churches in Banat region, Romania - part I, Procedia Struct. Integrity 44 (2023) 2058–2065, <https://doi.org/10.1016/j.prostr.2023.01.263>.

- [42] A. Lo Monaco, N. Grillanda, I. Onescu, M. Fofiu, F. Clementi, M. D'Amato, A. Formisano, G. Milani, M. Mosoarca, Seismic assessment of typical historical masonry churches in the Banat Region, Romania - Part II, *Procedia Struct. Integrity* 44 (2023) 2044–2051, <https://doi.org/10.1016/j.prostr.2023.01.261>.
- [43] M. Mosoarca, V. Gioncu, Failure mechanisms for historical religious buildings in Romanian seismic areas, *J. Cult. Herit.* 14 (3) (2013) e65–e72, <https://doi.org/10.1016/j.culher.2012.11.018>.
- [44] M. Mosoarca, I. Onescu, E. Onescu, A. Anastasiadis, Seismic vulnerability assessment methodology for historic masonry buildings in the near-field areas, *Eng. Fail. Anal.* 115 (2020), 104662, <https://doi.org/10.1016/j.engfailanal.2020.104662>.
- [45] M. Mosoarca, I. Onescu, E. Onescu, B. Azap, N. Chieffo, M. Sztar-Sirbu, Seismic vulnerability assessment for the historical areas of the Timisoara City, Romania, *Eng. Fail. Anal.* 101 (2019) 86–112, <https://doi.org/10.1016/j.engfailanal.2019.03.013>.
- [46] NTC, Rome: Ministry of Infrastructure and Transport, 2018.
- [47] I. Onescu, A. Lo Monaco, M. Fofiu, N. Grillanda, M. Mosoarca, M. D'Amato, G. Milani, A. Formisano, F. Clementi, Vulnerability Assessment of Historical Churches in Banat Seismic Region, Romania. In: *Proceedings of the SAHC Conference*. Tokyo, 2023.
- [48] M. A. Parisi, C. Chesi, P. Sferrazza, Damage Evolution in Churches Due to Repeated Earthquake Shocks. In: *16th ECEE Proceedings*, 2018, pp. 1–11. GRC.
- [49] F. Pavel, R.d. Vacareanu, K. Pitilakis, Preliminary Revision of the Seismic Zonation from the Current Romanian Seismic Design Code, in: *Earthquake Geotechnical Engineering for Protection and Development of Environment and Constructions*, CRC Press, 2019, pp. 4412–4449, <https://doi.org/10.1201/9780429031274>.
- [50] F. Pavel, R.d. Vacareanu, K. Pitilakis, Preliminary evaluation of the impact of Eurocode 8 draft revision on the seismic zonation of Romania, *Appl. Sci.* 12 (2) (2022) 649, <https://doi.org/10.3390/app12020649>.
- [51] F. Pavel, R.d. Vacareanu, K. Pitilakis, A. Anastasiadis, Investigation on site-specific seismic response analysis for Bucharest (Romania), *Bull. Earthq. Eng.* 18 (5) (2020) 1933–1953, <https://doi.org/10.1007/s10518-020-00789-0>.
- [52] A. Penna, C. Calderini, L. Sorrentino, C.F. Carocci, E. Cescatti, R. Sisti, A. Borri, C. Modena, A. Prota, Damage to churches in the 2016 Central Italy earthquakes, *Bull. Earthq. Eng.* 17 (10) (2019) 5763–5790, <https://doi.org/10.1007/s10518-019-00594-4>.
- [53] L. Piegl, W. Tiller, *The NURBS Book*, Springer Science & Business Media, 1996.
- [54] A. Preciado, A. Ramirez-Gaytan, J.C. Santos, O. Rodriguez, Seismic vulnerability assessment and reduction at a territorial scale on masonry and adobe housing by rapid vulnerability indicators: the case of Tlajomulco, Mexico, *Int. J. Disaster Risk Reduct.* 44 (April) (2020), 101425, <https://doi.org/10.1016/j.ijdrr.2019.101425>.
- [55] E. Ramirez, P.B. Lourenço, M. D'Amato, Seismic assessment of the Matera cathedral, In 1346–54 (2019), https://doi.org/10.1007/978-3-319-99441-3_144.
- [56] Romanian Design Code P100-1/, Ministry of Regional Development Public Administration and European Funds, 2013.
- [57] S. Ruggieri, C. Tosto, G. Rosati, G. Uva, G.A. Ferro, Seismic vulnerability analysis of masonry churches in Piemonte after 2003 Valle Scrivia earthquake: post-event screening and situation 17 years later, *Int. J. Arch. Heritage* 16 (5) (2022) 717–745, <https://doi.org/10.1080/15583058.2020.1841366>.
- [58] A.S. Araujo, P.B. Laurencu, D.V. Oliveira, J. Leite, Seismic assessment of St James church by means of pushover analysis – before and after the New Zealand earthquake, *Open Civil Eng. J.* 6 (1) (2012) 160–172, <https://doi.org/10.2174/1874149501206010160>.
- [59] N. Tarque, G. Camata, E. Spacone, H. Varum, M. Blondet, Numerical Modelling of In-Plane Behaviour of Adobe Walls. *Sísmica 2010*, 8th Congresso de Sismologia e Engenharia Sismica. CORE, 2010. <https://core.ac.uk/download/pdf/15566849.pdf>.
- [60] A. Tralli, A. Chiozzi, N. Grillanda, G. Milani, Masonry structures in the presence of foundation settlements and unilateral contact problems, *Int. J. Solids Struct.* 191–192 (2020) 187–201, <https://doi.org/10.1016/j.ijsolstr.2019.12.005>.
- [61] UNDRO, Natural Disasters and Vulnerability Analysis: Report of Expert Group Meeting, 9–12 July 1979, United Nations Disaster Relief Organisation, New York, 1979. <https://digitallibrary.un.org/record/95986>.
- [62] M. Valente, G. Milani, Damage assessment and partial failure mechanisms activation of historical masonry churches under seismic actions: three case studies in Mantua, *Eng. Fail. Anal.* 92 (2018) 495–519, <https://doi.org/10.1016/j.engfailanal.2018.06.017>.
- [63] J. Woessner, D. Laurentiu, D. Giardini, H. Crowley, F. Cotton, G. Grünthal, G. Valensise, et al., The 2013 European seismic hazard model: key components and results, *Bull. Earthq. Eng.* 13 (12) (2015) 3553–3596, <https://doi.org/10.1007/s10518-015-9795-1>.
- [64] T. Zsíros, Seismicity of the Bánát region, *Acta Geodaetica Geophys. Hungarica* 42 (3) (2007) 361–374, <https://doi.org/10.1556/AGeod.42.2007.3.8>.